Theory and application of the Day plot (M_{rs}/M_s versus H_{cr}/H_c) 1. Theoretical curves and tests using titanomagnetite data

David J. Dunlop

Geophysics, Physics Department, University of Toronto, Toronto, Ontario, Canada

Received 15 February 2001; revised 28 September 2001; accepted 4 October 2001; published 29 March 2002.

[1] Although most paleomagnetic and environmental magnetic papers incorporate a Day plot of the hysteresis parameters M_{rs}/M_s versus H_{cr}/H_c, a comprehensive theory covering superparamagnetic (SP), single-domain (SD), pseudo-single-domain (PSD), and multidomain (MD) (titano)magnetites is lacking. There is no consensus on how to quantify grain-size trends within the Day plot, how to distinguish MD from SP trends/mixtures, or whether magnetite, titanomagnetites, and other minerals have distinctive trends by which they might be identified. This paper develops the theory of the Day plot parameters for MD, MD + SD, PSD, and SP + SD grains of titanomagnetite ($Fe_{3-x}Ti_xO_4$) with compositions $x = 0$ (TM0 or magnetite) and $x = 0.6$ (TM60). MD grains have a separate trend that intersects the curve for SD + MD mixtures. SP + SD mixtures generate a variety of trends, depending on the SP grain size. All SP + SD curves lie much above those for MD or SD + MD trends, as has been proposed, but not demonstrated, previously. Data for PSD-size magnetites of many different origins fall along a single trend, but different levels of internal stress shift points for similar grain sizes along the "master curve." In order to use the Day plot to determine grain size, one must have independent information about the state of internal stress. Theoretical model curves for SD + MD mixtures match the PSD magnetite and TM60 data quite well, although the SD→MD transition region in grain size is much narrower for TM60 than for magnetite. The agreement between PSD data and SD + MD mixing curves implies that PSD behavior is due to superimposed independent SD and MD moments, either in individual or separate grains, and not to exotic micromagnetic structures such as vortices. The theory also matches M_{rs} and H_c values in mechanical mixtures of very fine and very coarse grains, although nonlinear mixing theory is required to explain some H_{cr} and H_{cr}/H_c data. *INDEX TERMS:* 1540 Geomagnetism and Paleomagnetism: Rock and mineral magnetism; 1594 Geomagnetism and Paleomagnetism: Instruments and techniques; 1533 Geomagnetism and Paleomagnetism: Remagnetization; 1512 Geomagnetism and Paleomagnetism: Environmental magnetism; *KEYWORDS:* hysteresis parameters, Day plot, magnetite, titanomagnetite, pseudo-single-domain grains, magnetic mixtures

1. Introduction

[2] A graph of the ratio of saturation remanence to saturation magnetization, M_{rs}/M_s, against the ratio of remanent coercive force to ordinary coercive force, H_{cr}/H_c, was proposed by *Day et al.* [1977], and further developed by *Parry* [1982], as a method of discriminating domain state (single-domain, SD; pseudo-single-domain, PSD; multidomain, MD) and, by implication, grain size. For Day et al.'s sized grains of titanomagnetite ($Fe_{3-x}Ti_xO_4$), values of the two ratios follow an approximately hyperbolic curve for all four compositions tested ($x = 0$, 0.2, 0.4, 0.6). There is a monotonic trend with grain size, the finer grains approaching SD endpoint values of M_{rs}/M_s and H_{cr}/H_c and the coarser grains approaching MD values. However, data for grains of the same size but different compositions lie on different parts of the curve. In addition, comparing the data of *Day et al.* [1977], *Parry* [1965, 1980, 1982], and *Dankers and Sugiura* [1981], different levels of internal stress introduced in sample preparation can be seen to shift points along the curve. In order to use the Day plot to determine grain size, one must therefore have independent information about mineral composition and state of internal stress.

0148-0227/02/2001JB000486$09.00

[3] Day plots have been published as part of many paleomagnetic and environmental magnetic studies, for suites of oceanic rocks [e.g., *Dunlop*, 1981; *Tauxe et al.*, 1996; *Gee and Kent*, 1999], soils and lake and marine sediments [e.g., *Özdemir and Banerjee*, 1982; *King et al.*, 1982; *Smirnov and Tarduno*, 2000], and continental carbonate rocks [e.g., *Jackson*, 1990; *Channell and McCabe*, 1994; *Suk and Halgedahl*, 1996]. These and many other data sets show that there is no single curve that explains all the data. *Jackson* [1990] proposed that the strikingly different trends for remagnetized and unremagnetized carbonate rocks result from mixtures of SP and SD grains in the first case and SD + MD mixtures in the second case. *Gee and Kent* [1999] likewise propose SP + SD and SD + MD mixtures as the cause of different trends observed in interior to rim traverses of submarine basalt pillows. *Tauxe et al.* [1996] numerically modeled SP + SD mixtures and were able to explain data for submarine basaltic glasses, which do not fall on any simple trend.

[4] The purpose of the present study is to make a first-principles theoretical treatment of the parameters M_{rs}, H_{cr}, H_c and their correlation in the Day plot for SP, SD, PSD, and MD grains and mixtures of these domain states. The theoretical predictions will then be compared to published data for magnetite and other titanomagnetites (particularly $Fe_{2.4}Ti_{0.6}O_4$ or TM60) with controlled grain sizes or mechanical mixtures of different sizes. In the companion paper by *Dunlop* [2002] the type curves will be

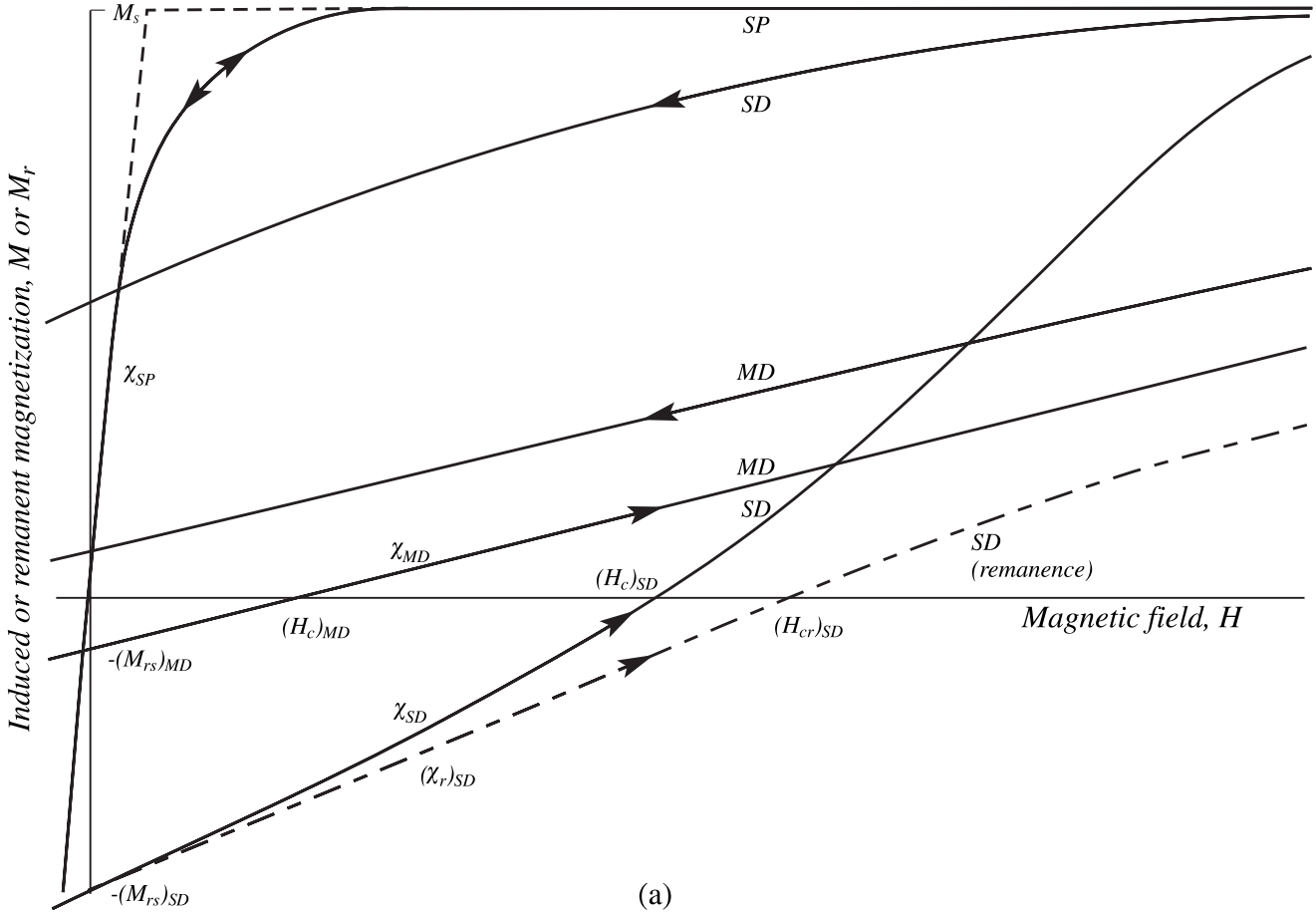

Figure 1. Model hysteresis curves for SP, SD, and MD grains. Symbols are defined in the text. (a) General *M*-*H* and M_r-*H* curves. (b) SD and two SP *M*-*H* curves for different SP fractions f_{SP}, showing the balance between SD and SP magnetizations when $H = H_c$. (c and d) *M*-*H* and M_r-*H* curves showing balance between SD and MD induced and remanent magnetizations at the critical fields H_c and H_{cr}.

compared to data for soils, sediments, carbonate rocks, and oceanic basalts and glasses.

2. Theory

2.1. SD and MD Limits

[5] Following *Day et al.* [1977], the M_{rs}/M_s versus H_{cr}/H_c diagram is usually divided into SD, PSD, and MD regions using SD and "true" MD values of the parameters to define the limits of the PSD region. For nonequidimensional grains of strongly magnetic minerals like magnetite, uniaxial shape anisotropy dictates an SD value $M_{rs}/M_s = 0.5$. Equidimensional SD grains of magnetite or TM60 have $M_{rs}/M_s = 0.866$ or 0.832 (negative and positive magnetocrystalline anisotropy, respectively). These values may be reduced by particle interactions, which are best assessed using Preisach or FORC diagrams [*Dunlop et al.*, 1990; *Pike et al.*, 1999; *Roberts et al.*, 2000]. H_{cr}/H_c for SD grains can range from 1.09 (single coercivity) to ≈2 (broad distribution of coercivities). Day et al. used $M_{rs}/M_s = 0.5$, $H_{cr}/H_c = 1.5$ as SD limits for titanomagnetites of all compositions.

[6] "True" MD behavior is defined to be full responsiveness of domains and domain walls to the internal demagnetizing field, $-N\mathbf{M}$ (N is demagnetizing factor), with no added SD-like component of magnetic remanence. In practice, the exact PSD-MD boundary has been difficult to determine experimentally. Day et al. assumed the values $M_{rs}/M_s = 0.05$, $H_{cr}/H_c = 4$ as MD limits, again for titanomagnetites of all compositions. The M_{rs}/M_s value is based on the well-known relationship, $M_{rs} = H_c/N$ (for details of this and other hysteresis relations, see *Dunlop and Özdemir* [1997, chapters 5 and 11]), substituting $H_c = 8$ kA/m (100 Oe), $N = 1/3$ ($4\pi/3$), $M_s = 480$ kA/m (480 emu/cm^3) for magnetite (cgs values in parentheses). Since different values apply for TM60, one would expect different MD limits for this mineral. Furthermore, $H_c = 8$ kA/m is a rather high coercive force for MD magnetite; the MD limit for this mineral may also be subject to revision (see section 2.2).

2.2. MD Distribution of M_{rs}/M_s and H_{cr}/H_c Values

[7] For larger MD grains, values of H_c are typically distributed downward from 8 kA/m to much smaller values. Therefore we can anticipate a distribution of M_{rs}/M_s and H_{cr}/H_c values as we move upward in grain size from the PSD-MD boundary. The MD saturation hysteresis loop (Figure 1a) consists of two offset linear branches with slope χ_{MD}. From the geometry, $\chi_{MD} = M_{rs}/H_c$. However, the "true" susceptibility χ_i, measuring the response of magnetization $\mathbf{M}$ to the internal field $\mathbf{H_i}$ (the applied field $\mathbf{H}$ minus the internal demagnetizing field $-N\mathbf{M}$) is much larger than χ_{MD} for strongly magnetic minerals like magnetite and TM60. The two susceptibilities are related by $\chi_{MD} = \chi_i (1 + N\chi_i)^{-1}$, where $(1 + N\chi_i)^{-1}$ is the screening factor due to self-demagnetization [see *Dunlop and Özdemir*, 1997, chapter 11]. Thus

$$M_{rs}/M_s = \chi_{MD} H_c/M_s = \chi_i (1 + N\chi_i)^{-1} H_c/M_s. \qquad (1)$$

When $\chi_i \gg \chi_{MD}$, $M_{rs} = H_c/N$, as given in section 2.1.

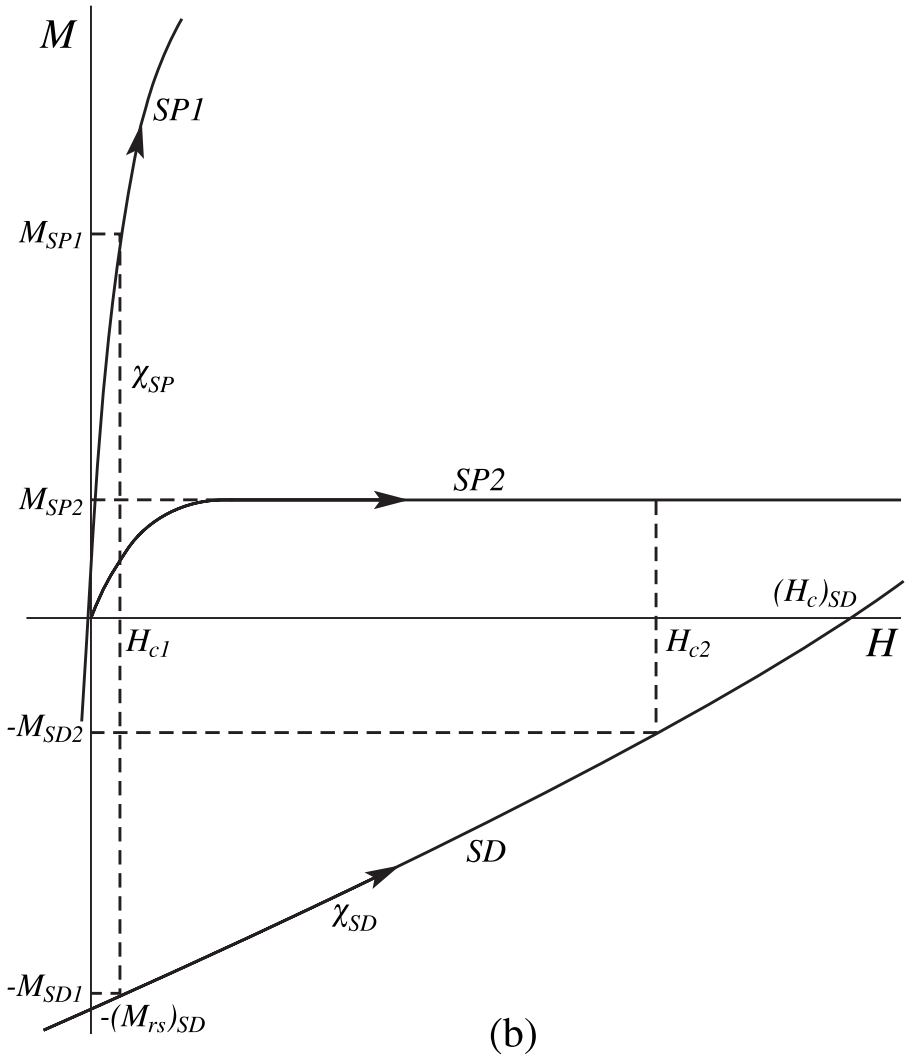

Figure 1. (continued)

[8] In exactly the same way, H_c is reduced compared to H_{cr} by self-demagnetization:

$$H_c = H_{cr}(1 + N\chi_i)^{-1} \tag{2a}$$

or

$$H_{cr}/H_c = (1 + N\chi_i). \tag{2b}$$

Combining (1), (2a), and (2b), we have

$$M_{rs}/M_s \times H_{cr}/H_c = \chi_i H_c/M_s = p. \tag{3}$$

Equation (3) defines a rectangular hyperbola on a Day plot of M_{rs}/M_s versus H_{cr}/H_c.

[9] The hyperbola constant p depends on mineral composition through M_s and on grain size and stress state (principally the density of dislocations, which impede domain wall motion) through χ_i and H_c. If the main mechanism of susceptibility and coercivity is domain wall motion within potential wells created by dislocations and other stress concentrations, χ_i and H_c are inversely related. For magnetite, M_s = 480 kA/m (or emu/cm^3). The exact value of $\chi_i H_c$ depends on the sizes and configurations of domains in a particular grain. A tentative theoretical value is $\chi_i H_c \approx 45$ kA/m [*Stacey and Banerjee*, 1974, equations (4.33) and (4.34)], which gives $p \approx 0.1$. This choice is supported by experimental data for magnetite over the grain size range 1.5–88 μm [*Parry*, 1965; *Stacey and Banerjee*, 1974, Table 4.1] and also, as section 3.5 will show, by a large body of other data for magnetite. An appropriate value of p for TM60 remains to be calculated.

2.3. Mixtures of SP and SD Grains

[10] *Tauxe et al.* [1996] numerically added entire SD and SP magnetization curves like those of Figure 1a to generate values of M_{rs}/M_s and H_{cr}/H_c for mixtures of SD and SP grains in various proportions. A simpler approach is the following. Between $-(M_{rs})_{SD}$ and $(H_c)_{SD}$, the SD hysteresis curve is approximately linear, with a slope $\chi_{SD} = (M_{rs})_{SD}/(H_c)_{SD}$ (Figure 1b). The SP magnetization curve is described by

$$M(H) = M_s L(\alpha) = M_s(\coth\alpha - 1/\alpha), \quad \alpha \equiv \mu_0 V M_s H/kT, \tag{4}$$

in which μ_0 is the permeability of free space ($4\pi \times 10^7$ H/m or 1 in cgs), V is grain volume, T is temperature in K, and k is Boltzmann's constant (1.38×10^{-23} J/K or 1.38×10^{-16} erg/K). The Langevin function $L(\alpha)$ saturates rapidly as α (i.e., H) increases. A linear approximation (shown dashed in Figure 1a), in which M increases with constant susceptibility $\chi_{SP} = \mu_0 V M_s^2/3kT$ (Curie's law) is

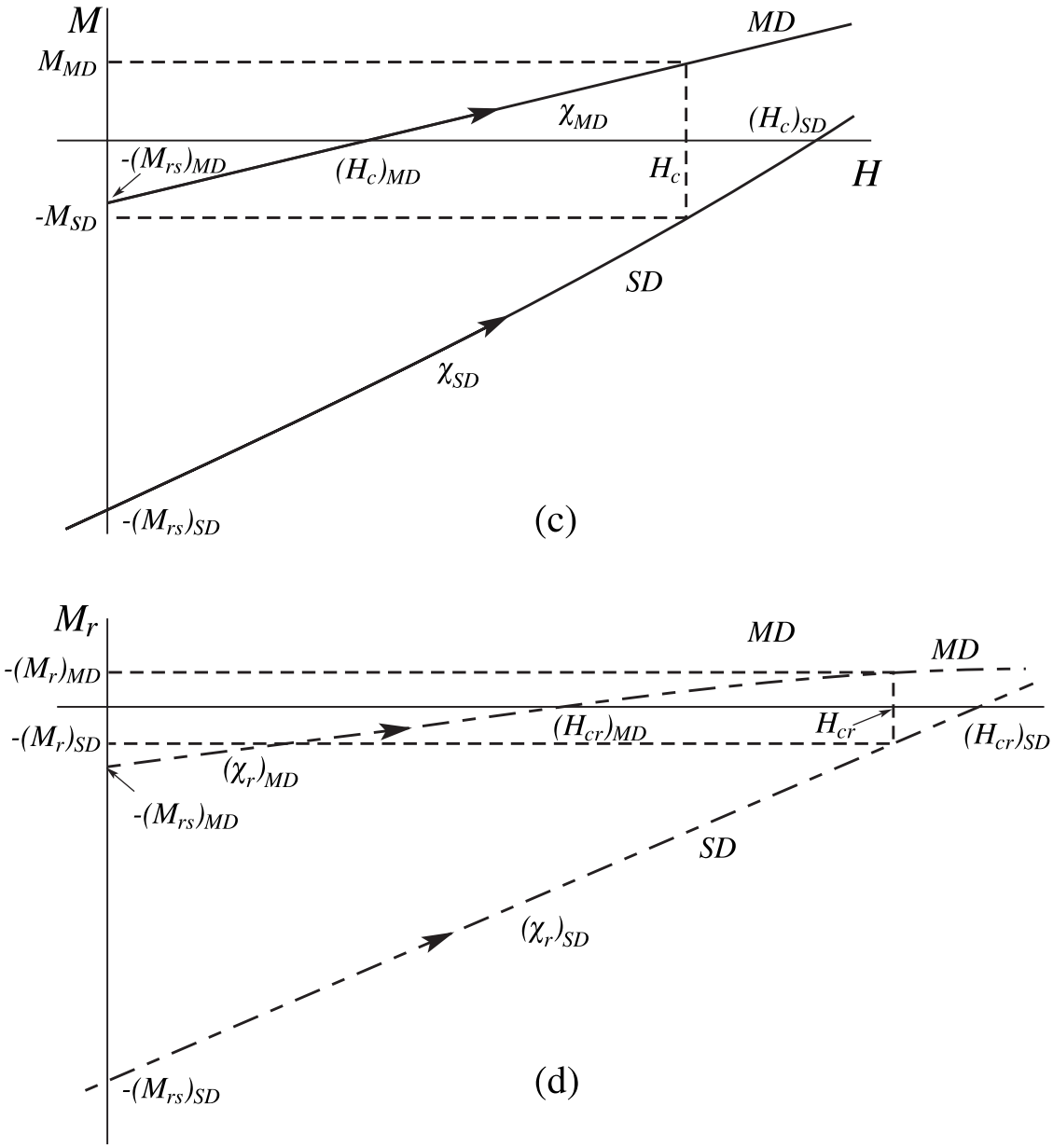

Figure 1. (continued)

often useful. (Tauxe et al. show that $M(H)$ is more complicated than a Langevin function when V approaches the size for stable SD behavior, but our calculations will be confined to smaller sizes.)

[11] The SP magnetization curve is reversible. M_{rs}, H_c, and H_{cr} are all zero. Thus in an SP + SD mixture we have that

$$M_{rs}/M_s = f_{SD}(M_{rs}/M_s)_{SD} \quad H_{cr} = (H_{cr})_{SD}, \tag{5}$$

where f_{SD} is the volume fraction of SD grains. H_c of the mixture is calculated as shown in Figure 1b. H_{c1} is the balance point field at which M_{SP1}, on the initial linear part of the SP1 magnetization curve, cancels $-M_{SD1}$ on the ascending SD hysteresis curve, giving zero net magnetization M. This balance is appropriate for a 50:50 mixture (i.e., $f_{SP} = f_{SD} = 0.5$) because the curves SD and SP1 have the same saturation magnetization M_s. A different balance applies if f_{SP} is considerably <50%, giving curve SP2. Then the balance point field H_{c2} is much larger than before and the SP magnetization M_{SP2} is saturated when the total magnetization $M_{SP2} - M_{SD2} = 0$.

[12] These two cases lead to distinct expressions for H_c of the mixture. If the SP magnetization is in the initial linear part of the $M(H)$ curve, then at $H = H_c$, $M = f_{SP}\chi_{SP}\ H_c - f_{SD}\ (M_{rs} - \chi_{SD}H_c) = 0$ (see Figure 1b). Rearranging, and noting that $M_{rs} = (M_{rs})_{SD} = \chi_{SD}\ (H_c)_{SD}$,

$$H_c = [f_{SD}\,\chi_{SD}/(f_{SD}\,\chi_{SD} + f_{SP}\,\chi_{SP})]\,(H_c)_{SD}, \tag{6}$$

(where χ_{SP} is initial slope, SP1) a volume-susceptibility weighted average. On the other hand, if the SP magnetization is saturated at $H = H_c$, $M = f_{SP}\,M_s - f_{SD}\ (M_{rs} - \chi_{SD}H_c) = f_{SP}\,M_s - f_{SD}\,M_{rs}\,[1 - H_c/(H_c)_{SD}] = 0$ (see Figure 1b), again using $M_{rs} = \chi_{SD}\ (H_c)_{SD}$. In this case,

$$H_c = \left[1 - (f_{SP}/f_{SD})/(M_{rs}/M_s)_{SD}\right]\,(H_c)_{SD} \tag{7}$$

(above SP saturation, SP2).

[13] A quick numerical test is to substitute $f_{SP} = f_{SD} = 0.5$ and Day et al.'s assumed SD values $(M_{rs})_{SD} = 0.5$, $(H_{cr}/H_c)_{SD} = 1.5$ in (5) and (6). Combining and rearranging, we have $(M_{rs}/M_s) \times (H_{cr}/H_c) = 0.5^2\ (1 + \chi_{SP}/\chi_{SD})\ 1.5$. Since $\chi_{SP} \gg \chi_{SD}$, $(M_{rs}/M_s) \times (H_{cr}/H_c) \gg 0.75$. The MD value for p (equation (3)) is ≈ 0.1. Therefore SP + SD curves will lie far above MD curves on a Day plot.

[14] One must first test which of (6) and (7) applies for a given mixture, i.e., whether H_c lies above or below SP saturation. Generally speaking, if f_{SP} is large, (6) will apply, and if f_{SP} is small, (7) will apply. There is a considerable region in which the Langevin curve deviates from the dashed lines in Figure 1a on which (6) and (7) are based. In this region, if $H = H_c$, $M = f_{SP} M_s L(\alpha_c) - f_{SD} M_{rs}\ [1 - H_c/(H_c)_{SD}] = 0$, and so

$$f_{SD}/f_{SP} = f_{SD}/(1 - f_{SD}) = \left[L(\alpha_c)/(M_{rs}/M_s)_{SD}\right] \cdot \left(1 - H_c/(H_c)_{SD}\right)^{-1}, \quad (8)$$

α_c being the value of α when $H = H_c$. The procedure for solution is to use a set of trial values for H_c and calculate f_{SD}, rather than vice versa. Once f_{SD} is known, M_{rs}/M_s follows from (5).

2.4. Mixtures of SD and MD Grains

[15] This situation is slightly more complicated than that of SP + SD mixtures because SD and MD grains both have remanences. The remanence ratio is a simple volume weighted average:

$$M_{rs}/M_s = f_{SD}\,(M_{rs}/M_s)_{SD} + f_{MD}\,(M_{rs}/M_s)_{MD}. \quad (9)$$

When $H = H_c$, $M = f_{SD}[-(M_{rs})_{SD} + \chi_{SD} H_c] + f_{MD}[-(M_{rs})_{MD} + \chi_{MD} H_c] = 0$ (see Figure 1c). Since $(M_{rs})_{SD} = \chi_{SD}\ (H_c)_{SD}$ and $(M_{rs})_{MD} = \chi_{MD}\ (H_c)_{MD}$, we have that

$$H_c = \left[f_{SD}\,\chi_{SD}(H_c)_{SD} + f_{MD}\,\chi_{MD}(H_c)_{MD}\right] / (f_{SD}\,\chi_{SD} + f_{MD}\,\chi_{MD}). \quad (10)$$

If the ascending SD and MD remanence curves can also be approximated as linear, with slopes $(\chi_r)_{SD}$ and $(\chi_r)_{MD}$, respectively (Figure 1d), then from the definition of remanent coercive force, when $H = H_{cr}$, $M_r = f_{SD}[-(M_{rs})_{SD} + (\chi_r)_{SD}\ H_{cr}] + f_{MD}[-(M_{rs})_{MD} + (\chi_r)_{MD} H_{cr}] = 0$. However, $(M_{rs})_{SD} = (\chi_r)_{SD}\ (H_{cr})_{SD}$ and $(M_{rs})_{MD} = (\chi_r)_{MD}\ (H_{cr})_{MD}$, giving

$$H_{cr} = \left[f_{SD}\,(\chi_r)_{SD}\,(H_{cr})_{SD} + f_{MD}\,(\chi_r)_{MD}\,(H_{cr})_{MD}\right] / \left[f_{SD}\,(\chi_r)_{SD} + f_{MD}\,(\chi_r)_{MD}\right]. \quad (11)$$

[16] SD + MD mixtures have been considered by previous authors. Equations (11) and (12) of *Hodych* [1990] are equivalent to (9) and (10). However, the equations derived by *Parry* [1980, equations (A6) and (A7), 1982, equation (3)] for H_c of mixtures do not match (10) above unless the susceptibilities of coarse and fine grains are equal. This is approximately true if the coarse and fine fractions are both of MD size. It is not true if the fines are of SD size because usually $\chi_{SD} > \chi_{MD}$ (Figures 1a and 1c). *Parry* [1980, equation (A11)] gives an equation for H_{cr} of mixtures, assuming $(\chi_r)_{SD} = (\chi_r)_{MD}$ (contrary to Figure 1d). It also involves internal field susceptibilities and demagnetizing factors, which cannot be directly measured. Because of these limitations, Parry's equations are not recommended.

[17] H_{cr} of an SD + MD mixture is generally $\gg (H_{cr})_{MD}$ (see Figure 1d). In this field range the MD remanence curve can be significantly nonlinear. *Nagata and Carleton* [1987, equation (10)] proposed that $M_r \propto H$, when $H \le (H_{cr})_{MD}$ but $M_r \propto 1/H$, when $H \ge (H_{cr})_{MD}$. Adapting their equations to the remanence curve ascending from $-(M_{rs})_{MD}$, as in Figure 1d, we have

$$M_r = \left\{\left[H/(H_{cr})_{MD}\right] - 1\right\}\,(M_{rs})_{MD}, \quad 0 \le H \le (H_{cr})_{MD} \quad (12a)$$

$$M_r = \left\{1 - \left[(H_{cr})_{MD}/H\right]\right\}\,(M_{rs})_{MD}, \quad H \ge (H_{cr})_{MD} \quad (12b)$$

Analogous equations apply to the SD remanence curve.

[18] Since the balance field H_{cr} is $< (H_{cr})_{SD}$ but $> (H_{cr})_{MD}$, we are in the linear part of the SD curve but the non-linear part of the MD curve when $H = H_{cr}$ (Figure 1d). The net remanence $M_r = (M_r)_{MD} - (M_r)_{SD} = 0$ at $H = H_{cr}$, and so

$$f_{MD}\,(M_{rs})_{MD}\left\{1 - \left[(H_{cr})_{MD}/H_{cr}\right]\right\} + f_{SD}(M_{rs})_{SD} \cdot \left\{\left[H_{cr}/(H_{cr})_{SD}\right] - 1\right\} = 0. \quad (13)$$

This nonlinear equation for H_{cr} is most easily solved by trial and error.

2.5. Pseudo-Single-Domain Grains

[19] Pseudo-single-domain (PSD) behavior was postulated by *Stacey* [1962] as an explanation of the transitional magnetic properties of magnetite over a broad grain size range between SD and truly MD. Proposed microscopic origins of PSD behavior include [*Dunlop*, 1998] (1) mixtures of MD and metastably SD grains [*Halgedahl and Fuller*, 1983]; (2) permanent SD-like moments in MD grains, e.g., domain wall moments [*Dunlop*, 1977], imbalance moments of irregularly shaped grains [*Fabian and Hubert*, 1999]; (3) surface moments, e.g., closure domains, which change substantially with changes in body domain structure [*Stacey and Banerjee*, 1974; *Özdemir et al.*, 1995]; and (4) exotic micromagnetic structures unlike either classic SD or MD structures, e.g., vortex and double-vortex states [*Williams and Dunlop*, 1995; *Fabian et al.*, 1996].

[20] Micromagnetic simulation of hysteresis behavior has so far been limited to a few model grain sizes below 1 μm, leaving most of the PSD size range unexplored. No hysteresis modeling has been carried out for surface domains, but like body domains, they must be highly responsive to internal demagnetizing fields. Metastable SD grains and intrinsic SD-like moments, on the other hand, are easy to model. They represent simple mixtures of SD and MD moments, either in separate grains or as independent responses of individual grains. Thus data for titanomagnetites of PSD size are compared tentatively in section 3.5 to theoretical curves from SD + MD equations (9)–(11) and (13).

3. Results

3.1. Calculations of Day Plot Curves

[21] Theoretical Day plot curves for magnetite (Figure 2) were calculated using (3) with $p = 0.1$ (solid line) or $p = 0.15$ (dashed line) for MD grains, (5)–(8) for mixtures of SP and SD grains, and (9)–(11) for mixtures of SD and MD grains (tentative model for PSD grains). Reference SD values chosen were $M_{rs}/M_s = 0.5$ (uniaxial shape anisotropy), $H_{cr}/H_c = 1.25$ (see section 2.1). Details of the calculations are given in sections 3.2–3.6.

[22] The remanence and coercivity ratios of SP-SD mixtures are greatly affected by the SP grain size. The smaller the size, the smaller is the SP susceptibility χ_{SP} in equation (4) and the lower the curves lie on the Day plot. However, even the lowest curve calculated, for 10-nm SP grains, lies much above MD curves, in a region not explored by *Day et al.* [1977]. High values of H_{cr}/H_c correspond to small values of H_c, for which (6) is appropriate. Depending on grain size, lower values of H_{cr}/H_c may mean large enough values of H_c that the Langevin function saturates. Equation (7) is then used, generating the common SP saturation envelope in Figure 2. Exact Langevin calculations improve only slightly on the two-segment approximation for 10-nm SP grains.

[23] For grain sizes larger than 15 nm, all curves are shown dashed because the SP magnetization curve is no longer a simple Langevin function [*Tauxe et al.*, 1996]. This region calls for nonlinear numerical modeling. However, in the companion

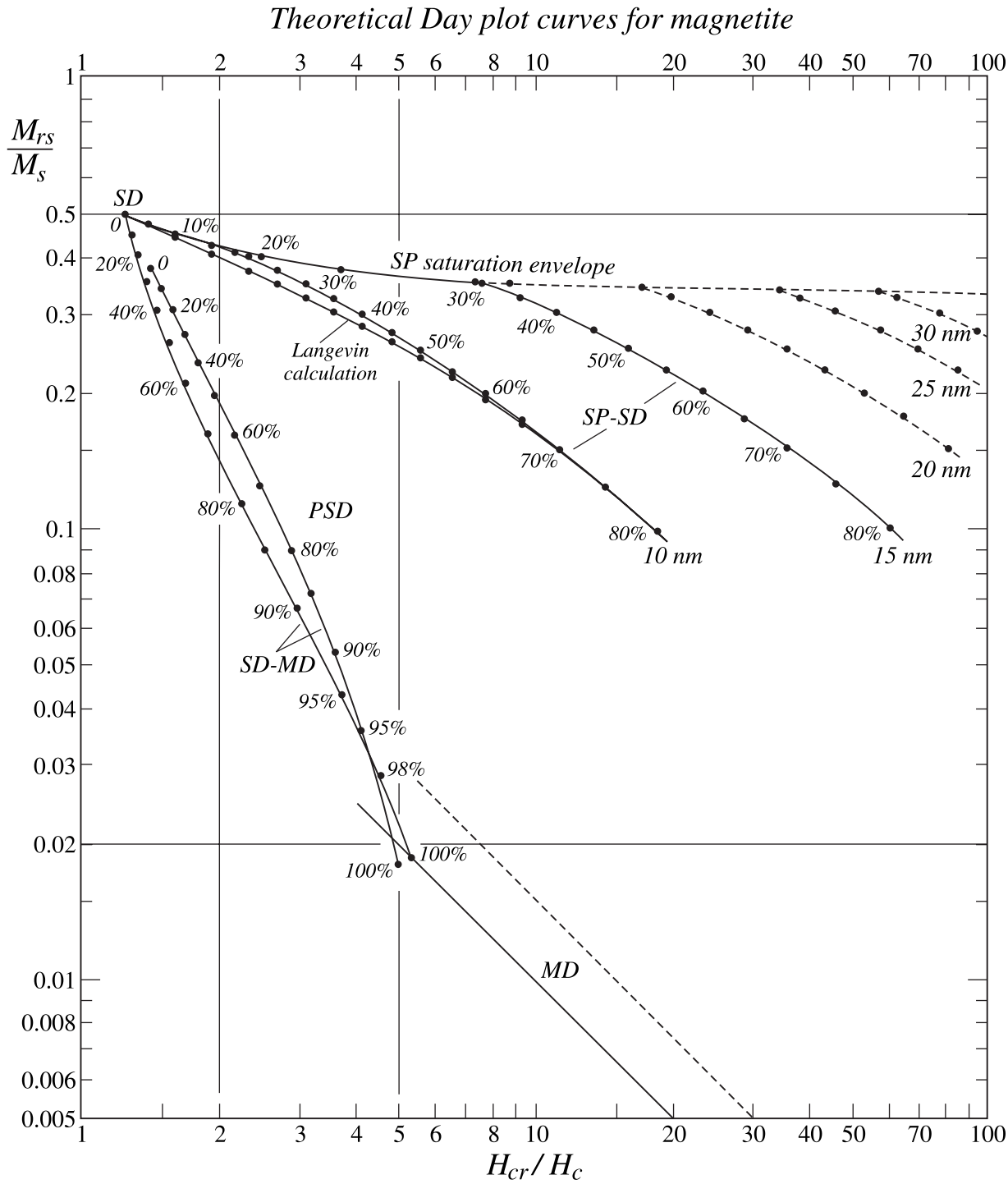

Figure 2. Theoretical Day plot curves calculated for magnetite using the equations developed in section 2. Detailed explanations of individual curves are given in the text. Numbers along curves are volume fractions of the soft component (SP or MD) in mixtures with SD grains.

paper by *Dunlop* [2002], actual published data sets are confined to the region of the solid curves, where Langevin modeling is valid.

[24] The two SD-MD curves shown in Figure 2 are based on mixing calculations between SD and MD endpoint values of two different data sets, as explained in section 3.5. The boundary between these "PSD" curves and the theoretical MD curve for magnetite (using $p = 0.1$) is different from the conventional one. *Day et al.* [1977] used $M_{rs}/M_s = 0.05$, $H_{cr}/H_c = 4$ as MD limits (see section 2.1). The present work suggests $M_{rs}/M_s = 0.02$, $H_{cr}/H_c = 5$ as boundary values between PSD and MD regions. In addition, a new region with $M_{rs}/M_s > 0.1$ and H_{cr}/H_c values as high as 100 is seen to be associated with mixtures of SP and SD grains.

3.2. Theory and Experiment in the MD Region

[25] Data for MD magnetites by many authors are compared to the prediction of (3) in Figure 3. Data from *Rahman et al.*

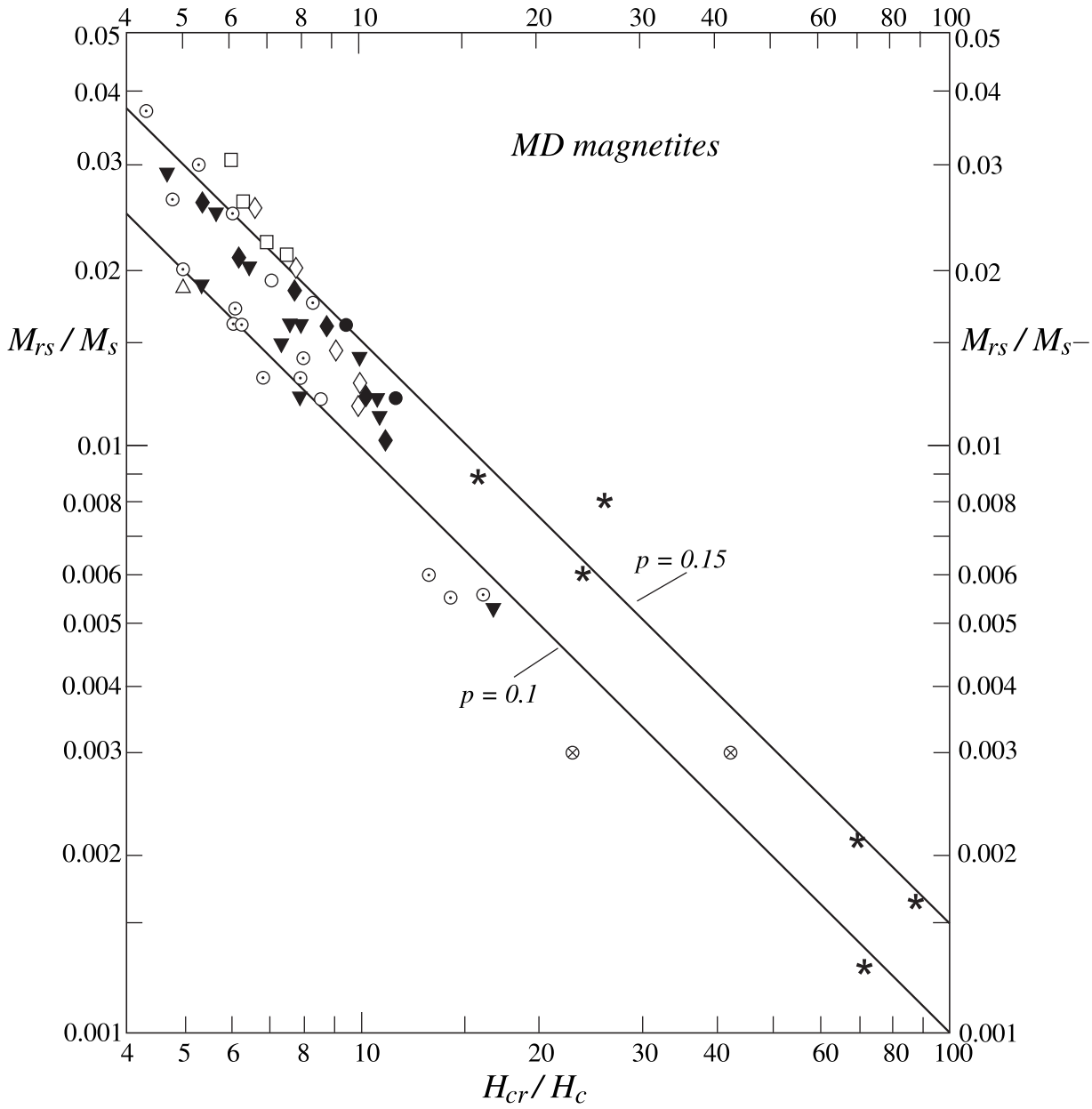

Figure 3. Day plot for MD magnetites. Data sources are as follows: open circles with dots, *Rahman et al.* [1973]; open triangle, *Day et al.* [1977]; inverted solid triangles, *Parry* [1965, 1980]; open and solid diamonds, *Dankers and Sugiura* [1981], unannealed and annealed; open squares, *Hartstra* [1982]; open and solid circles, D. J. Dunlop and S. Xu (unpublished data, 1999), unannealed and annealed; stars, *Heider et al.* [1987, 1996]; open circles with crosses, *Özdemir and Dunlop* [1997, 1998]. The line with $p = 0.1$ has theoretical backing; the line with $p = 0.15$ does not but forms a natural upper bound to the data.

[1973] on crushed grains, from *Heider et al.* [1987, 1996] on hydrothermal grains, and from *Özdemir and Dunlop* [1997, 1998] on large single crystals extend the data set to $0.001 < M_{rs}/M_s < 0.01$, $10 < H_{cr}/H_c < 100$, allowing the theory to be tested over a very broad region. Equation (3) with $p = 0.1$ gives a reasonable first-order fit to most of the data. A second line with $p = 0.15$ (for which there is no a priori justification) is an upper bound to the data.

3.3. Theory and Experiment for SP + PSD Mixtures

[26] There are no published data for controlled mixtures of SP and SD grains, except in abstract form [*Carter and Moskowitz*, 1999]. However, if SD is replaced by PSD, (5)–(8) describe SP + PSD mixtures, for which unpublished data have kindly been made available by B. Moskowitz. The SP component is a ferrofluid (a suspension of ≈10-nm magnetite particles, Ferrofluidics MO1) and the PSD component is a 1- to 3-μm synthetic magnetite (Wright 3006). H_c of the PSD end-member is well below the SP saturation field, and so (6) or (8) was used to calculate H_c of the mixture. The two equations gave essentially identical results.

[27] Most of the data are bracketed by theoretical curves with SP particle sizes of 9.3 and 10 nm (Figure 4). Only for mixtures with 10% and 25% SP material do the data fall somewhat off the curves. The M_{rs}/M_s values for these mixtures agree with (5) but H_c as predicted by (6) or (8) gives higher than observed values of

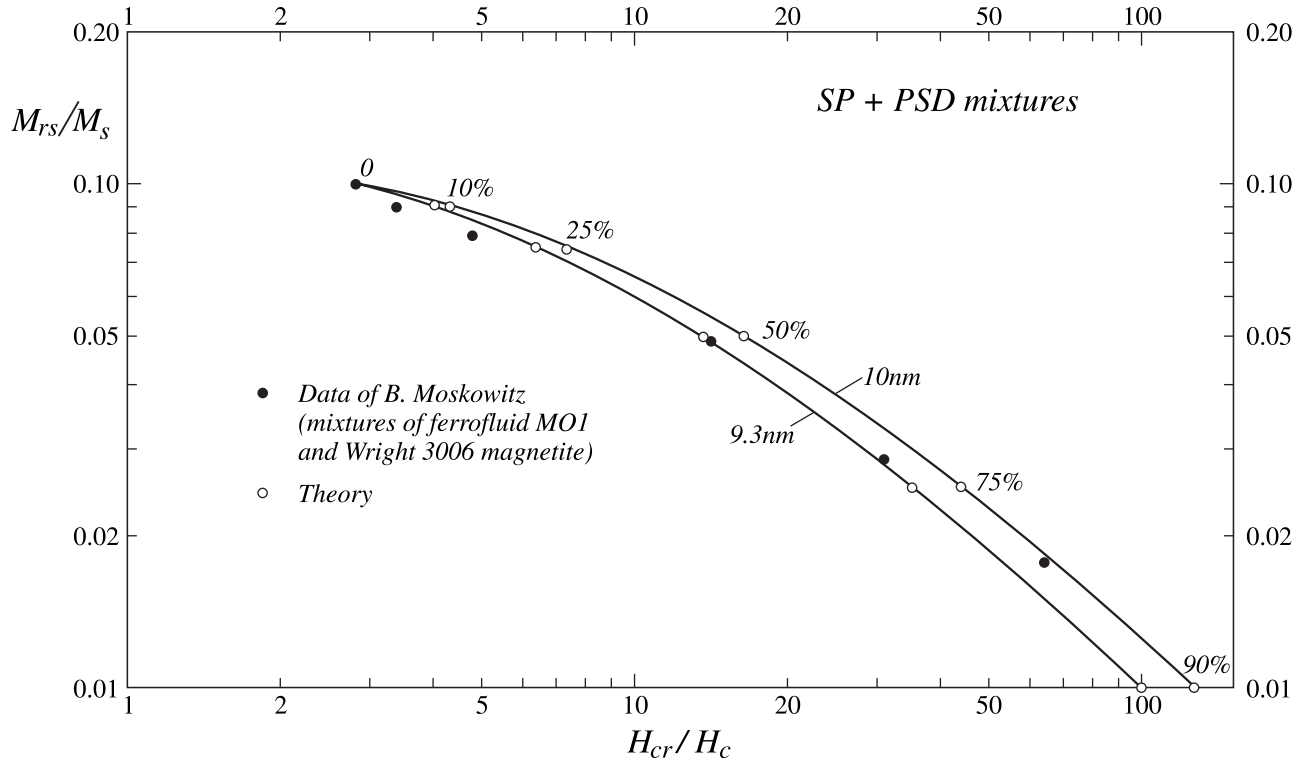

Figure 4. Experimental data for mixtures of SP and PSD magnetites compared to theoretical curves generated by using (6) or (8) for H_c and substituting H_{cr} and M_{rs}/M_s values of the PSD end-member (Wright 3006 magnetite) for $(H_{cr})_{SD}$ and $(M_{rs}/M_s)_{SD}$ in (5). Numbers along the curves are SP volume fractions f_{SP}.

H_{cr}/H_c. No reasonable value for SP particle size can explain these two data points.

3.4. Theory and Experiment for SD + MD and PSD + MD Mixtures

[28] M_{rs}/M_s, H_c, H_{cr}, and H_{cr}/H_c data for mechanical mixtures of fine and coarse magnetite or TM60 grains in various proportions permit individual tests of the mixing relations (9), (10), (11), and (13). Data for PSD + MD mixtures of 4.5- and 220-μm magnetites [*Parry*, 1980] are compared with theory in Figure 5. As predicted, M_{rs}/M_s values increase linearly with f_f (the fraction of the fine-grained component, analogous to f_{SD} in (9)). The predicted H_c function is slightly curved because the values χ_f and χ_{MD} substituted in (10) for the 4.5- and 220-μm magnetites differ by ~15%. The H_c data follow the curve quite closely. The theoretical H_{cr} and H_{cr}/H_c functions are much more strongly curved because the remanence susceptibilities $(\chi_r)_f$ and $(\chi_r)_{MD}$ ($=M_{rs}/H_{cr}$) are different by a factor 6. Equation (11), which assumes a linear MD remanence curve, fits the data only approximately. Equation (13), which incorporates the nonlinear remanence curve (equations (12a) and (12b)), gives a near-perfect fit to the data.

[29] Data for mixtures of elongated SD (ESD) and 220-μm MD magnetites, with high resolution for SD volume fractions ≤6% [*Parry*, 1982], are matched with theory in Figure 6. The ESD particles are surface oxidized and have M_s values ≈20% less than those of the 220-μm magnetites. Under these circumstances, (9) must be replaced by the nonlinear equation

$$M_{rs}/M_s = \left[f_{SD}\,(M_{rs})_{SD} + f_{MD}(M_{rs})_{MD}\right] \Big/ \left[f_{SD}\,(M_s)_{SD} + f_{MD}\,(M_s)_{MD}\right], \quad (14)$$

which is appropriate for any mixture of minerals with different M_s values. The M_{rs}/M_s variation predicted by (14) is curved downward, in the same fashion as the data but less strongly. The H_c data are well described by (10), but (11) is inadequate in explaining the H_{cr} data when the SD fraction is small. Equation (13) (nonlinear MD remanence curve) gives a much closer fit. Notice that the H_{cr}/H_c data and the nonlinear theoretical curve both pass through a peak for nonzero values of f_{SD}. Such a peak is a general feature when $(\chi_r)_{SD}$ and $(\chi_r)_{MD}$ values are very different [*Nagata and Carleton*, 1987]; in this case, they differ by a factor 15.

[30] H_c and H_{cr} data for mixtures of SD (0.11 μm) and MD (140 μm) TM60 grains [*Day et al.*, 1977] are compared to the predictions of (10), (11), and (13) in Figure 7. The H_c data follow a strongly convex-down curve, which is well described by linear mixing theory (equation (10)). The strong curvature results from the sevenfold contrast between SD and MD susceptibilities. Since the remanent susceptibilities differ by only a factor 2, linear mixing theory for H_{cr} (equation (11)) generates a less strongly curved function, which however totally fails to match the data. Nonlinear mixing theory (equation (13)) predicts a completely different function, strongly convex upward, which fits the H_{cr} data fairly well except when f_{SD} is below ~15%. The strong curvature in this case is caused by the very different (by a factor of 17) SD and MD H_{cr} values: In mixtures the MD remanence curve is pushed to high fields, much beyond its linear region (compare Figure 1d).

3.5. Theory and Experiment for PSD Grains of Magnetite

[31] In Figure 8, nine published M_{rs}/M_s versus H_{cr}/H_c data sets for magnetites in the PSD size range are compared with the predictions of SD + MD mixing theory. Mixing curve 1 has as its MD and SD end-members 131-μm magnetite synthesized by the ceramic method and 0.11-μm material produced by wet grinding (WG) the coarse material [*Day et al.*, 1977]. Mixing curve 2 has as its coarse end-member grains prepared by crushing natural massive magnetite and separating a fraction with mean size 21 μm

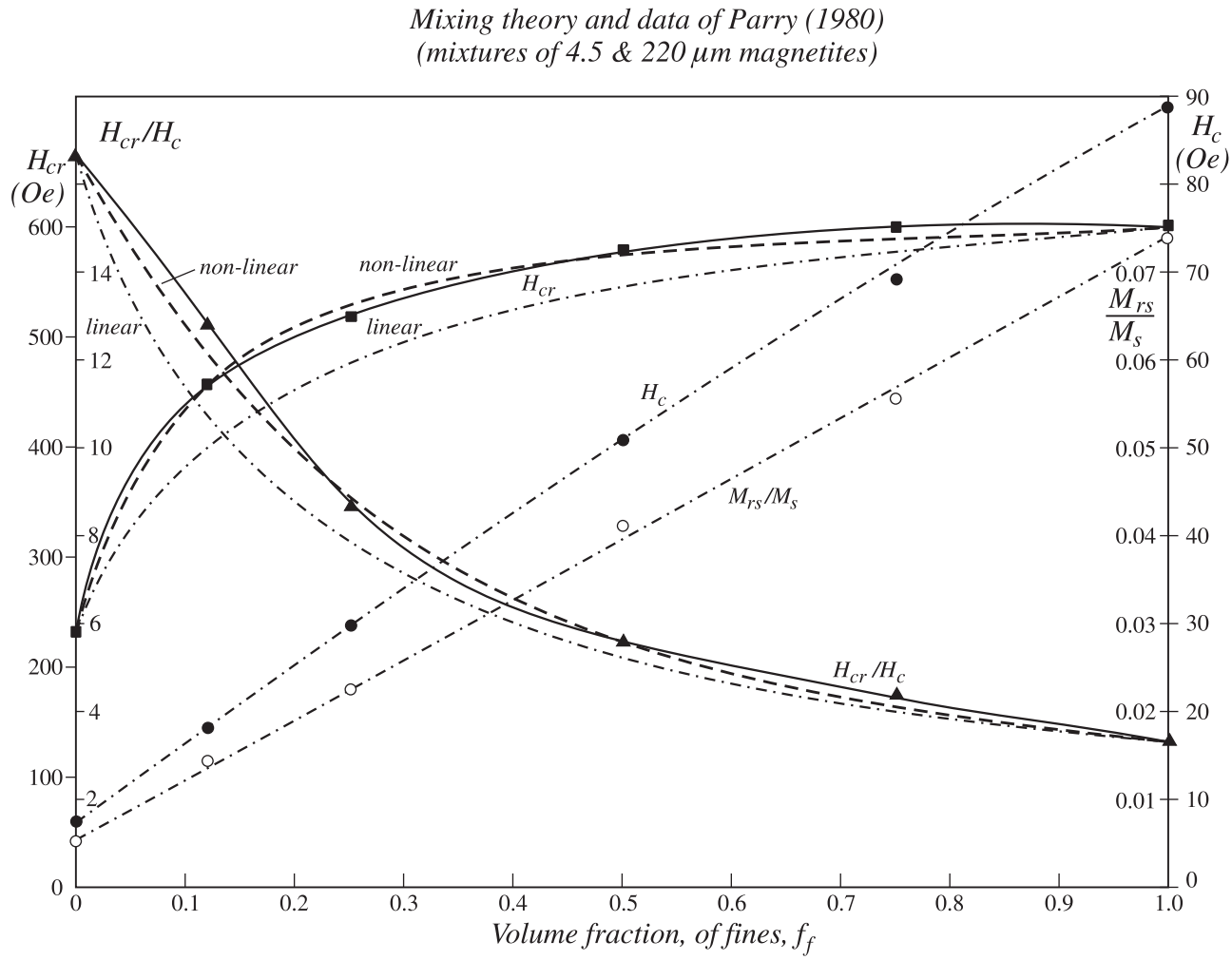

Figure 5. Experimental data (circles, squares, and triangles, joined by solid curves) for mixtures of 4.5- and 220-μm magnetites [*Parry*, 1980] compared with theoretical predictions of (9) for M_{rs}/M_s, (10) for H_c, and (11) or (13) for H_{cr} (linear and nonlinear approximations, dot-dashed and dashed curves, respectively).

[*Parry*, 1965]. Parry's magnetites did not include any very SD-like sample, and so a hypothetical SD end-member with $M_{rs}/M_s = 0.5$ and $H_{cr}/H_c = 1.25$ was assumed for calculations (Table 1).

[32] The nine data sets are plotted together in Figure 8a and shown separately in Figures 8b–8e. It is clear from Figure 8a that all the PSD magnetite data are fairly well accounted for by mixing curves 1 and 2. Deviations from the curves are comparable to scatter of data within a particular data set. It is also immediately apparent that within any particular data set, there is a monotonic trend of more SD-like M_{rs}/M_s and H_{cr}/H_c values with decreasing grain size but that values for a particular grain size do not match between data sets. For example, values for ≈20-μm grains are spread along a considerable section of the curves, and values for 0.76- to 1.5-μm magnetites of different origins span the middle one third of the curves.

[33] A case in point are the data in Figure 8b. The 0.085-μm chemically produced and 0.076-μm hydrothermal magnetites have M_{rs}/M_s values of 0.4 and 0.25, respectively. The M_{rs}/M_s values of the 0.25-μm chemical and 0.22-μm hydrothermal magnetites differ by a factor 2. The hydrothermal magnetite crystals have narrow size distributions and regular shapes and are unstrained. The chemical magnetites are likely to have broader size distributions, irregular particle shapes, and higher strains. One or more of these factors must be responsible for the shift in M_{rs}/M_s and H_{cr}/H_c toward more SD-like values for the chemical magnetites and more MD-like values for the hydrothermal magnetites.

[34] The data sets of *Parry* [1965, 1980] are featured in Figure 8c. The two sample suites were produced by crushing massive natural magnetites of different provenances, then annealing the different size fractions to reduce strains produced by the crushing. The data sets agree fairly well with each other and with the theoretical curves.

[35] The two suites of magnetites in Figure 8d were crushed from the same starting material, millimeter-size natural magnetite crystals, but one set was annealed for several hours at 700°C to reduce internal strains while the other set was left unannealed. The annealing temperature was too low to produce any significant grain growth by sintering. The displacement of the points for unannealed samples toward more SD-like values of M_{rs}/M_s and H_{cr}/H_c must be due to the higher internal strains and resulting stresses in unannealed grains compared with annealed grains of the same size.

[36] Unannealed magnetites crushed from synthetic [*Day et al.*, 1977] and natural [*Hartstra*, 1982] coarse-grained starting material are compared in Figure 8e. The natural unannealed data points agree quite closely with the corresponding unannealed sample data in Figure 8d. The agreement is not as close, but still reasonable, between data points for synthetic and natural samples of similar size in Figure 8e. State of internal strain/stress is a more important factor determining the position of PSD data on the Day plot than the source of the starting magnetite.

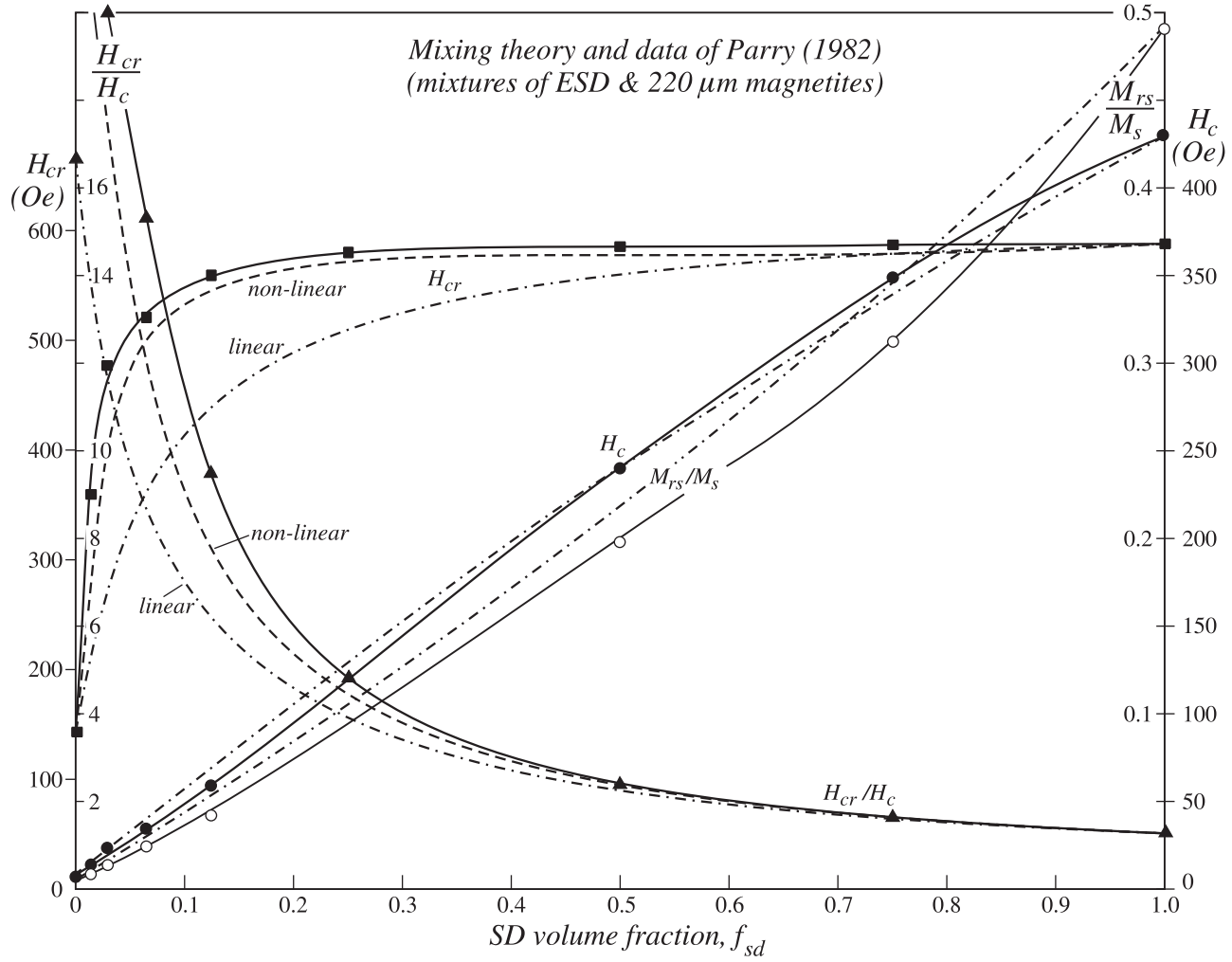

Figure 6. Experimental data for mixtures of elongated SD (surface oxidized) and 220 μm (unoxidized) magnetite grains [*Parry*, 1982] compared to theoretical curves generated as in Figure 5. In this case, H_{cr}/H_c values for some of the mixtures are higher than H_{cr}/H_c values for the pure end-members, and nonlinear theory is necessary to explain the H_{cr} and H_{cr}/H_c data. Solid curves join experimental points; theoretical curves are dot-dashed (linear) or dashed (nonlinear).

3.6. Data and Theoretical Curves for Intermediate-Size Titanomagnetites

[37] Data for titanomagnetites of compositions x = 0, 0.2, 0.4 and 0.6 were plotted as a single set by *Day et al.* [1977] and appeared to delineate a single trend independent of composition. When plotted separately (Figure 9), however, the different compositions have distinct trends. The theoretical SD + MD mixing model of section 2.4 fits the magnetite (x = 0) data quite well, as we saw also in Figure 8e. However, the same mixing model, using parameters of the fine (F) and coarse (C) end-members of other compositions, predicts curves that do not fit the data at all. Furthermore, there is a suggestion in the data of an increasingly steep descent in M_{rs}/M_s values as the x value increases. That is, the SD → MD transition becomes sharper and the PSD or transitional region becomes narrower.

[38] Figure 10 illustrates data for TM60 (x = 0.6) from three different studies. The descent in M_{rs}/M_s is abrupt and the (M_{rs}/M_s, H_{cr}/H_c) data do not follow, even approximately, a hyperbolic relation. Nor do they follow the upwardly convex mixing curve between coarse and fine end-members. A mixing calculation using end-members closer together in grain size does fit the intermediate points (for Day et al.'s data, but not very well for the other data) and emphasizes the sharpness of the SD → MD transition. The PSD effect, or broad transitional region between SD and MD behavior, which is so evident in magnetite, is almost absent in TM60.

4. Discussion

4.1. Theory and Type Curves

[39] To use either the linear or nonlinear theories for mixtures, one need only know the values of M_s, M_{rs}, H_c, and H_{cr} for SD or MD end-members and χ_{SP} for an SP end-member. Since χ_{SP} is strongly volume dependent (equation (4)), the SP particle size must be known. Conversely, once the type curves for SP + SD mixtures have been tested (which remains to be done), inversion of data for unknown mixtures to determine the average SP particle size is straightforward.

[40] The theory can readily be extended to mixtures of three or more phases. Unlike the situation for binary mixtures, however, unmixing real data is not simple. Fairly complete magnetization type curves (remanent as well as induced) are then necessary. The more components in the mixture, the more detailed must be the knowledge of the individual magnetization curves [*Thompson*, 1999].

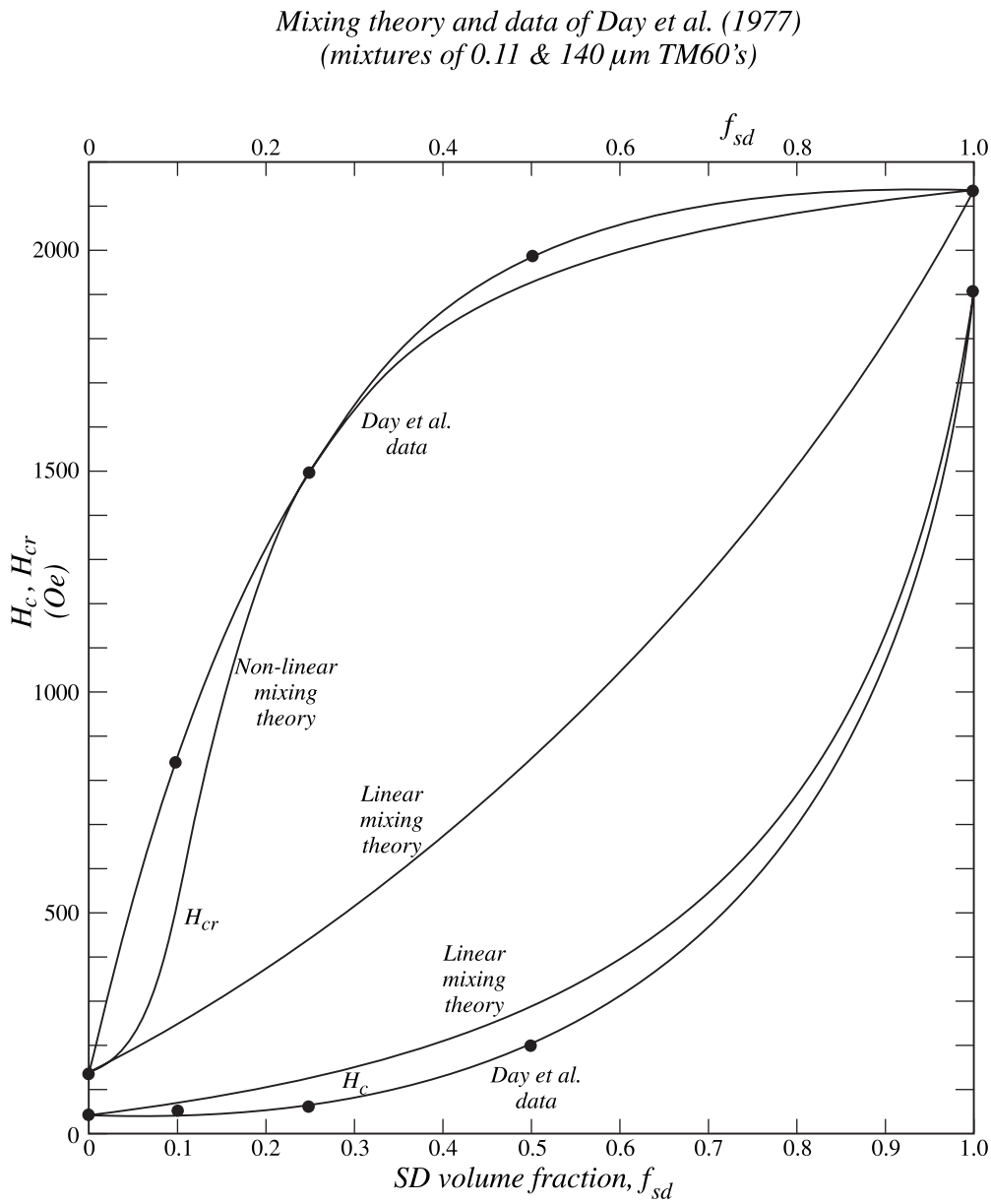

Figure 7. Experimental data for mixtures of 0.11 μm and 140 μm TM60 grains [*Day et al.*, 1977] compared to theoretical curves generated as in Figure 5. Linear mixing theory can explain the H_c data but not the H_{cr} data.

4.2. Distribution of Points for MD, PSD, and SP + SD Grains

[41] Several previously unrecognized features of the Day plot emerge from the present theory and its fit to data sets for titanomagnetites of controlled grain size.

1. MD grains have a broad range of possible values, distributed linearly on a log-log plot, from $M_{rs}/M_s \approx 0.02$, $H_{cr}/H_c \approx 5$ to $M_{rs}/M_s \approx 0.001$, $H_{cr}/H_c \approx 100$ (Figure 3). With decreasing grain size, M_{rs}/M_s tends to increase and H_{cr}/H_c tends to decrease. The determining factor is H_c, not grain size per se. M_{rs}/M_s is proportional to H_c (equation (1), noting that $\chi_i/(1 + N\chi_i) \approx$ const) and H_{cr}/H_c is inversely proportional to M_{rs}/M_s (equation (3) with $\chi_i H_c$ = const). Thus lower H_c (or higher χ_i) will displace points in the MD region to smaller M_{rs}/M_s and larger H_{cr}/H_c. The density of dislocations and other sources of domain wall pinning or nucleation play a role as important as grain size.

2. Within the PSD region, data for magnetites of controlled sizes follow SD + MD mixing curves quite closely (Figures 8a, 8b, 8c, 8d, and 8e). On a log-log Day plot these trends are not linear, as some authors have assumed in fitting their data sets, nor do they have the same average slope as the linear MD trend (Figure 2). The PSD and MD trends intersect at an angle of 20° or so. Higher or lower internal stress levels displace points along the curves in the same fashion as in the MD region (Figures 8b and 8d).

3. When SP grains form part of the mixture of phases, the curves are even more nonlinear on a log-log Day plot (Figure 2). Linear regression fits to data for SP mixtures or linear projections of data sets are not appropriate. The only available data set (SP + PSD) is reasonably well fit by theory, although the data are somewhat less arcuate in their trend than the curves (Figure 4). The fits predict quite a precise value of 9–10 nm for the average SP particle size.

4.3. Bimodal Mechanical Mixtures

[42] A curious feature of the data for mechanical mixtures of two populations of grains with very different domain states and hysteresis parameters is that H_{cr}/H_c for the mixed phases is sometimes larger than H_{cr}/H_c for either pure end-member (e.g., Figures

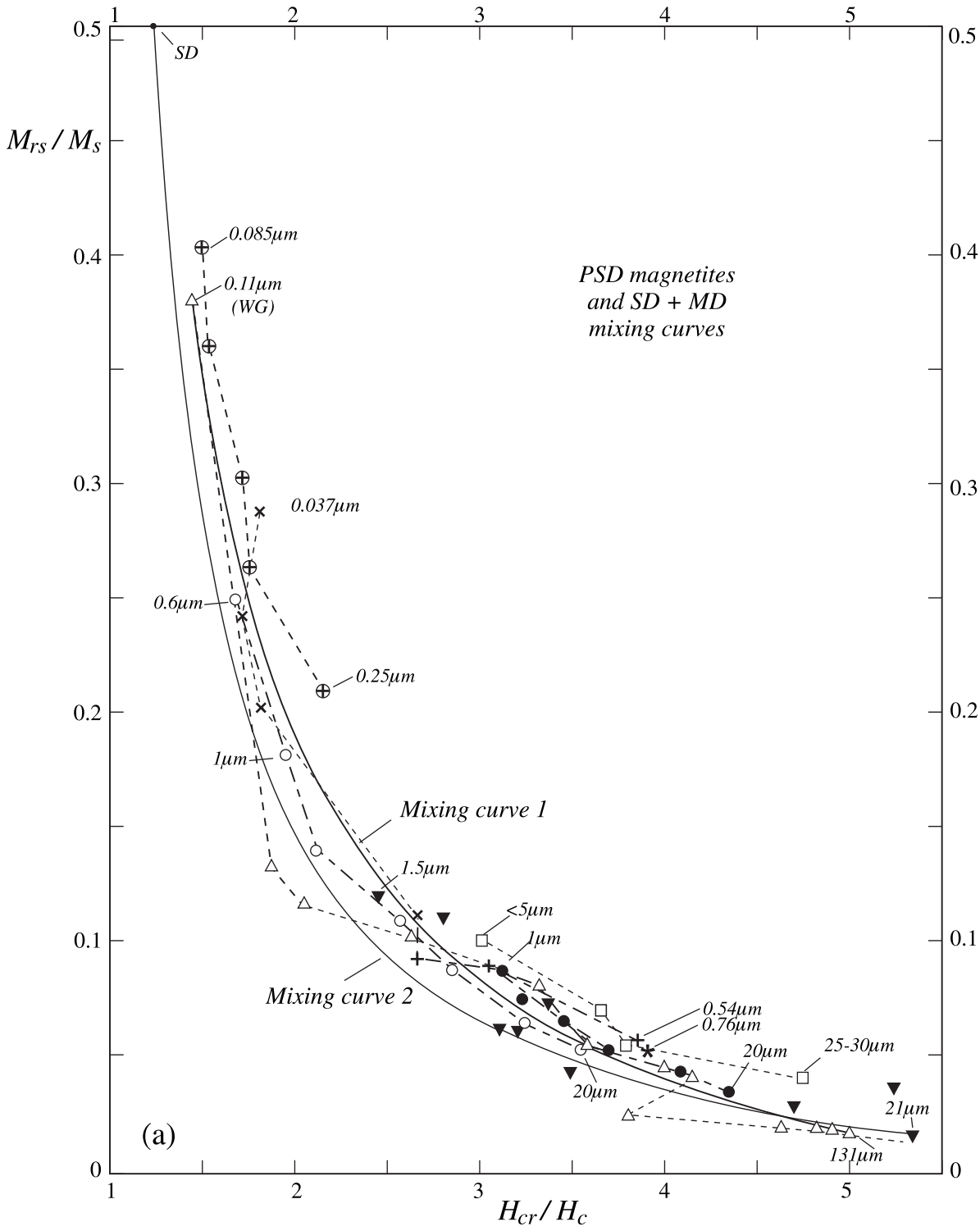

Figure 8. Comparison of experimental data for sized PSD magnetites and theoretical SD + MD mixing curves calculated using (9)–(11)) with coarse- and fine-grained end-member data from *Day et al.* [1977] and *Parry* [1965] (mixing curves 1 and 2, respectively). Data source are as follows: circles with crosses, *Schmidbauer and Schembera* [1987], *Schmidbauer and Keller* [1996]; open triangles, *Day et al.* [1977]; crosses, *Dunlop* [1986]; open (solid) circles, D. J. Dunlop and S. Xu (unpublished data, 1999), unannealed (annealed); inverted solid triangles, *Parry* [1965, 1980]; pluses, *Argyle and Dunlop* [1990]; open squares, *Hartstra* [1982]; star, *Heider et al.* [1987, 1996]. (a) To first order, PSD data are explained as due to simple mixtures of SD and MD moments. (b) An enlarged view of the data for chemically and hydrothermally produced magnetites. (c) Enlarged view of the data for *Parry*'s [1965, 1980] annealed crushed magnetites. (d) Enlarged view of the data for Dunlop and Xu's annealed and unannealed magnetites. (e) Enlarged view of the data for two sets of unannealed crushed magnetites. *Day et al.*'s [1977] magnetites were synthetic, while *Hartstra* [1982] magnetites were natural.

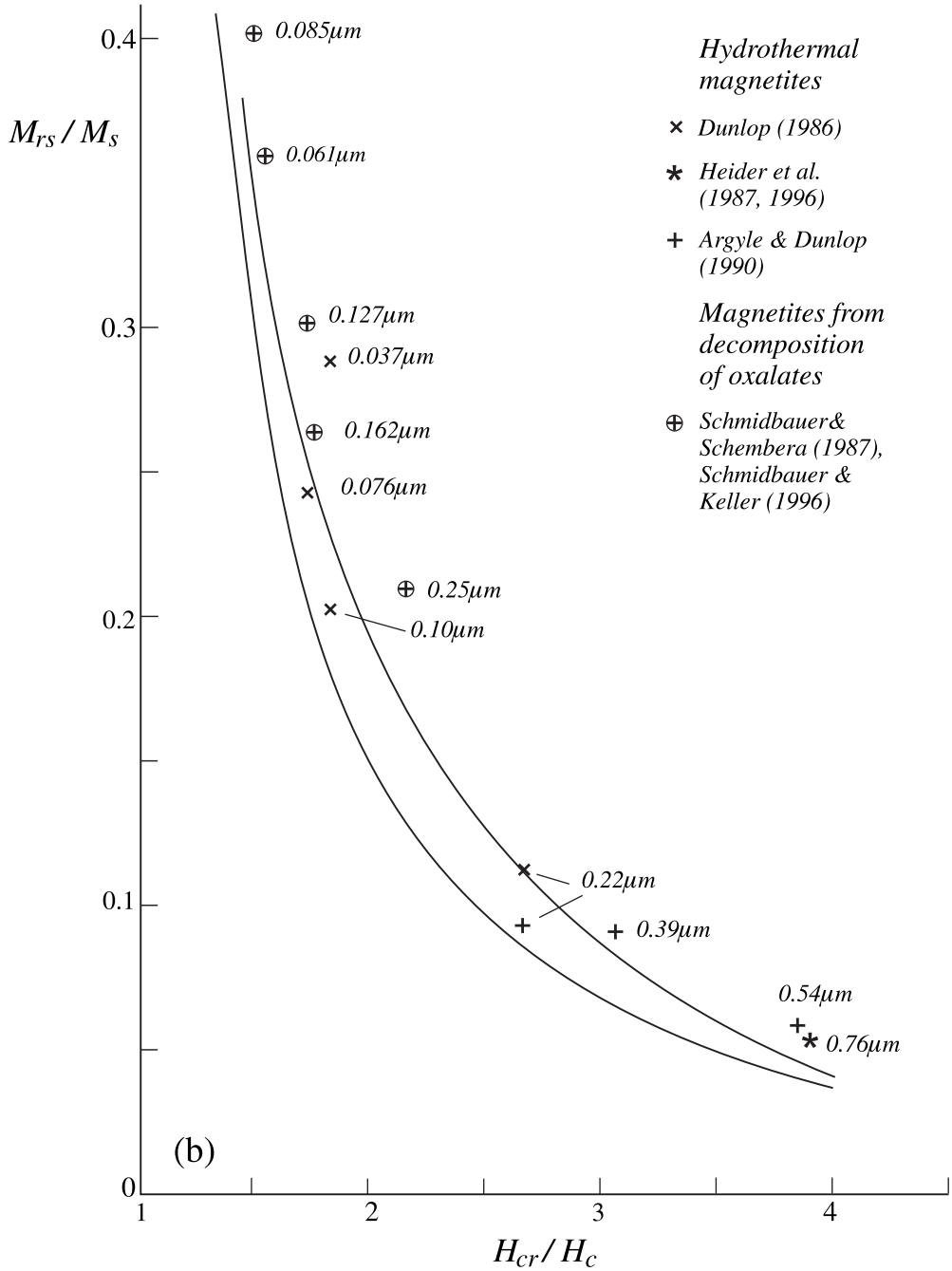

Figure 8. (continued)

6 and 11). The explanation is that H_{cr}/H_c of the mixture is not a weighted average of H_{cr}/H_c values of the pure phases. Rather it is the ratio of very differently weighted individual averages of H_{cr} and H_c. H_{cr} is dominated by the magnetically hard phase because $(\chi_r)_{SD} \gg (\chi_r)_{MD}$. H_c is fairly neutrally weighted ($\chi_{SD} \approx \chi_{MD}$) in magnetite but biased toward the soft phase ($\chi_{SD} \ll \chi_{MD}$) in TM60. The biasing is clear in Day et al.'s H_{cr} and H_c data for TM60 (Figure 7). The ratio tends to peak for small fractions (5–25%) of the hard phase where H_c is small but H_{cr} is rising sharply toward the hard-phase value. (A related phenomenon is wasp-waisted hysteresis loops of mixed hard and soft phases [*Roberts et al.*, 1995; *Tauxe et al.*, 1996].)

[43] The H_{cr}/H_c data are not particularly well explained by theory (Figure 11). Day et al.'s data for mixtures of 0.11- and 131-μm magnetites peak at an H_{cr}/H_c value twice that of the soft phase when ≈20% of the hard phase is present. In this case, the variation of H_{cr} with SD volume fraction is well matched by linear theory (equation (11)), but H_c is not explained by (10), and no peak is predicted in the H_{cr}/H_c data (linear mixing theory 1). Decreasing χ_{SD} to the measured initial susceptibility rather than using the ascending main loop susceptibility (linear mixing theory 2) does produce a peak, but it is quite small (Figure 11a).

[44] In the case of Day et al.'s TM60 mixtures, linear mixing theory is a complete failure, as was seen also in Figure 7. Nonlinear theory (equation (13) for H_{cr}) produces a peak in H_{cr}/H_c that is about one-half the observed peak and shifted to lower f_{SD} (Figure 11b).

[45] On a Day plot the H_{cr}/H_c and M_{rs}/M_s data for bimodal mixtures fall in a novel region to the right of the PSD data for magnetite or the 1.7- to 16-μm transitional data for TM60 (Figure 12). The deviation of points for binary mixtures from the

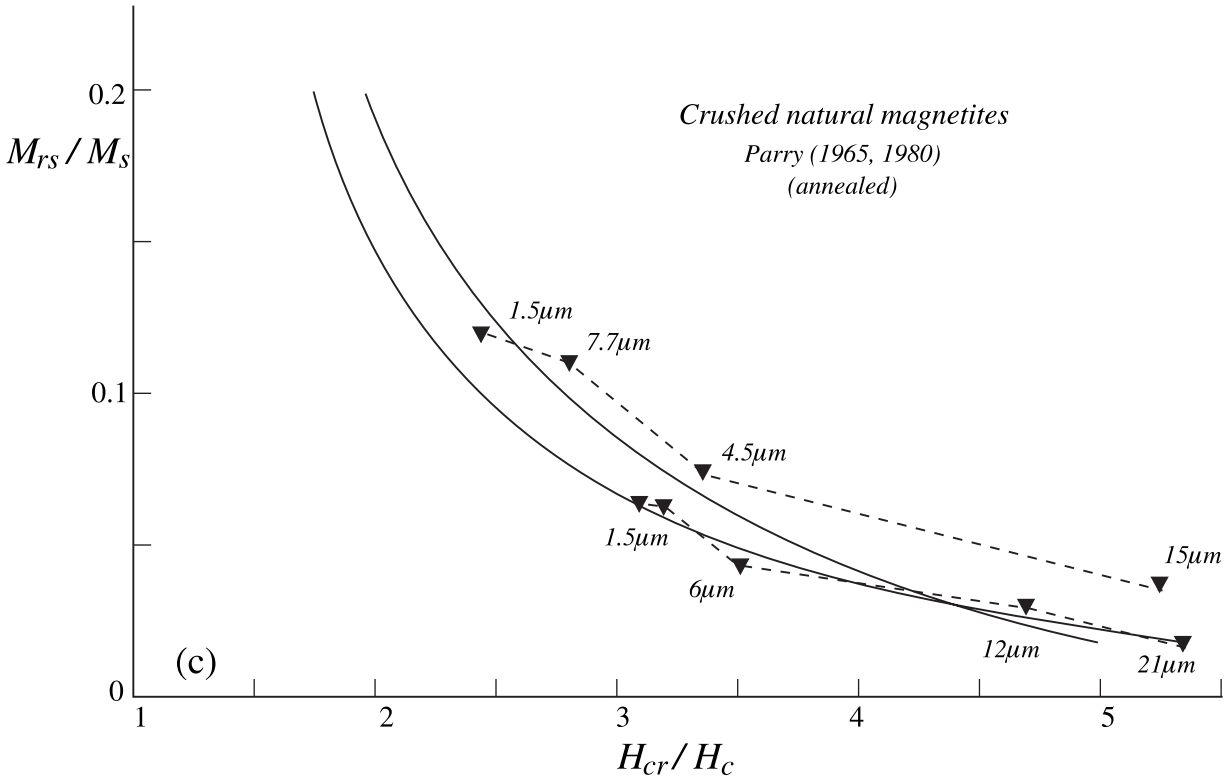

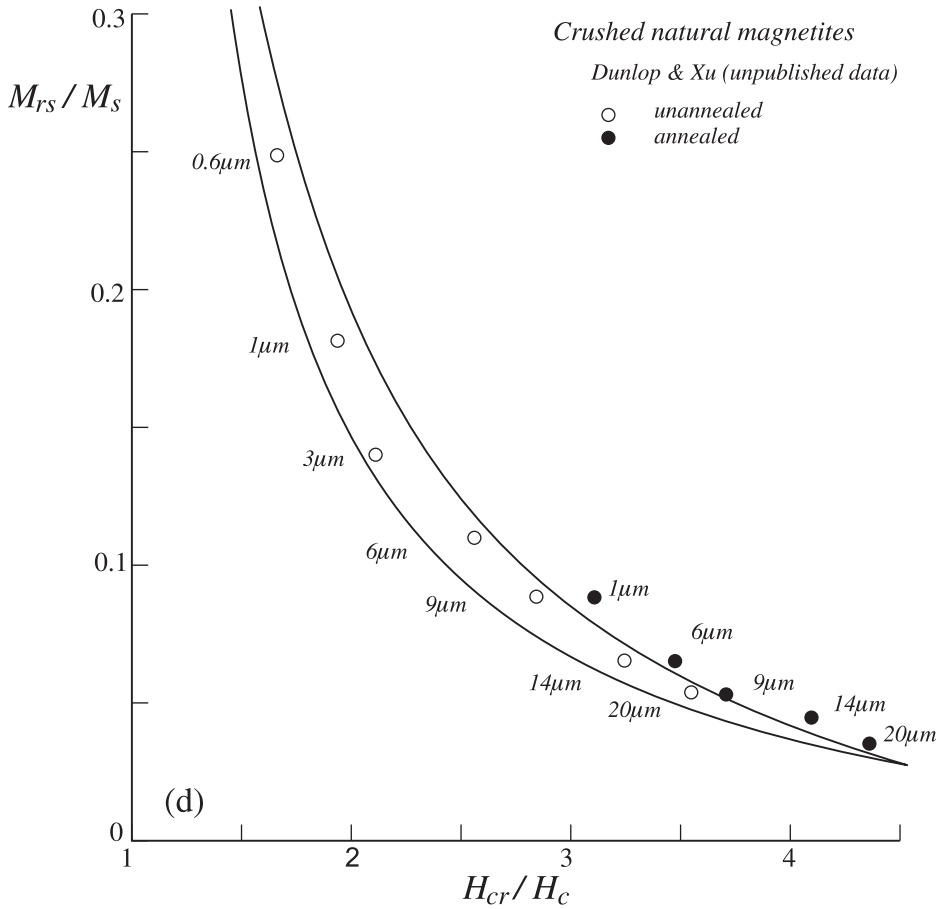

Figure 8. (continued)

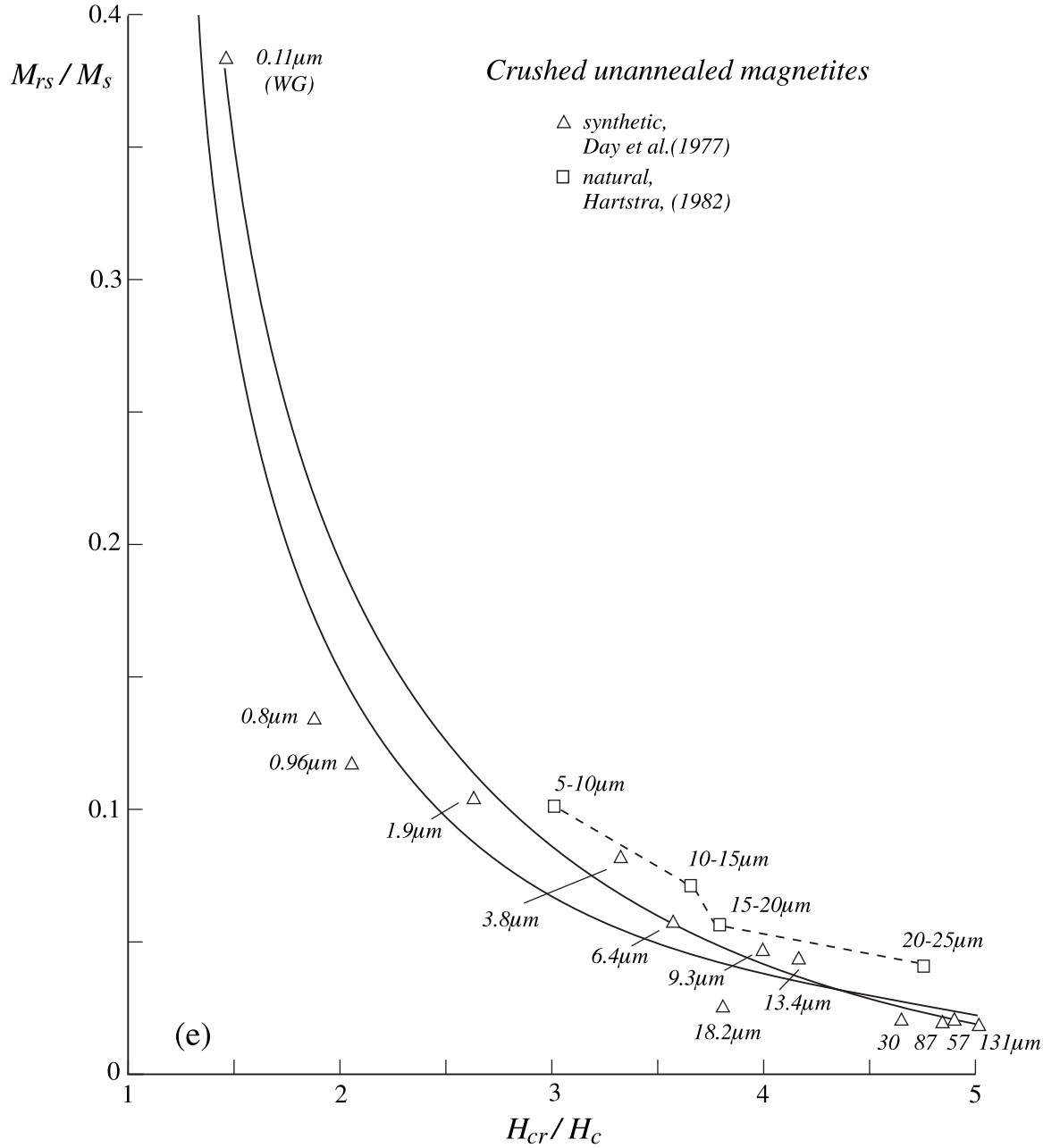

Figure 8. (continued)

data trend for grains of a single size is highly variable and depends on the contrast between susceptibilities and coercivity values of the hard and soft phases. In the case of magnetite (Figure 12a), *Day et al.*'s [1977] data deviate the most, *Parry*'s [1982] data (one set of two plotted) deviate less, and *Parry*'s [1980] data (not plotted; see Figure 5) are compatible with the PSD curves.

[46] The diagnostic value of the Day plot turns on the narrowness of the trends (e.g., Figure 2). Bimodal mixtures complicate matters. Their data points scatter across a broad area between the narrow bands occupied by data for PSD and MD grains on the one hand and SP + SD mixtures on the other. In paper 2, we will see that few actual data for rocks fall in this intermediate region but those that do cannot be interpreted unambiguously.

4.4. Significance of the PSD Data Trend for Magnetite

[47] Day plot data sets for narrowly sized magnetites in the PSD range follow curves (labeled 1 and 2 in Figure 8a) based on linear mixing theory (equations (9)–(11)). No PSD data fall in the bimodal mixtures region of Figure 12a, implying that PSD hysteresis can be described by a mixture of SD-like and MD-like moments, but the SD and MD susceptibilities and coercivities do not differ excessively.

[48] On the basis of the values of χ, χ_r, H_c, and H_{cr} for SD and MD end-members used in calculating mixing curves 1 and 2 (Table 1), H_c values differing by a factor 10 are tolerable if χ values differ by no more than a factor 3, and χ_r values an order of magnitude different are allowable if H_{cr} endpoint values are no more than a factor 3 different. These contrasts are typical for magnetite. More extreme contrasts, e.g., between ESD and 100- or 220-μm magnetites in *Parry*'s [1982] mixtures, produce deviations from the linear mixing curves into the bimodal region of Figure 12a. These are unlikely in nature unless there are two different sources of magnetite in a rock.

[49] SD and MD TM60 grains can have much greater contrasts in coercivities and susceptibilities than SD and MD magnetite

Table 1. Values of Magnetic Parameters for Fine-Grained and Coarse-Grained End-members Used in SD Plus MD Linear Mixing Calculations for Magnetite[a]

Parameter	SD1	MD1	SD2	MD2
M_{rs}/M_s	0.380	0.019	0.500	0.019
H_c, Oe	396	32	400	43
H_{cr}, Oe	565	160	500	230
χ (= M_{rs}/H_c)	0.465	0.288	0.600	0.209
χ_r (= M_{rs}/H_{cr})	0.326	0.058	0.480	0.039

[a] Mixing curve 1 of Figure 8 used data for 0.11-μm WG magnetite (SD1) and 131-μm magnetite (MD1) from *Day et al.* [1977, Tables II and III]. Mixing curve 2 used hypothetical SD values (SD2) and *Parry*'s [1965] data for 21-μm magnetite (MD2).

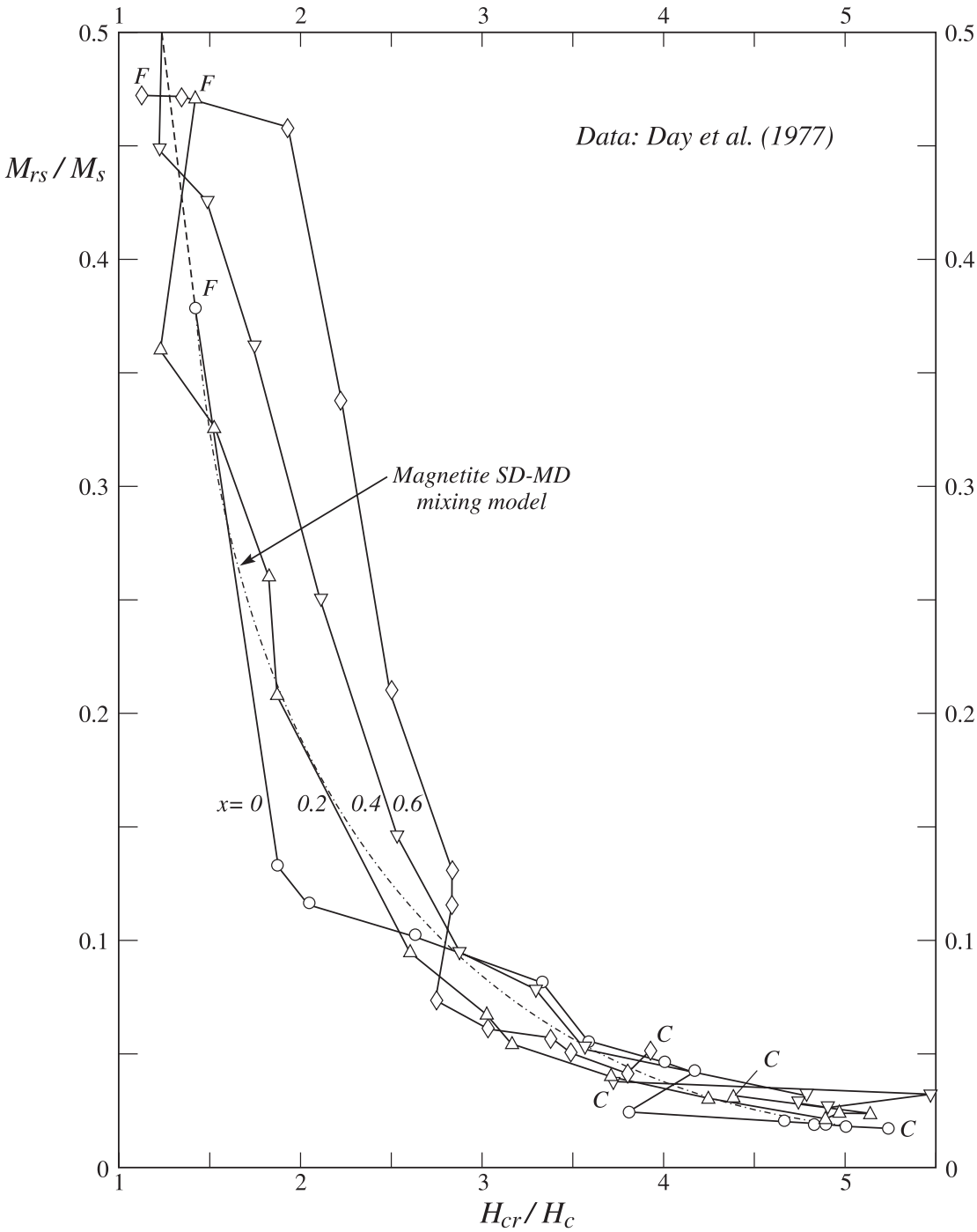

Figure 9. *Day et al.*'s [1977] data for sized titanomagnetites plotted as four separate sets for different titanium compositions *x*. C and F indicate the coarse- and fine-grained end-members of each set. The different compositions have separate subparallel data trends, not a single trend.

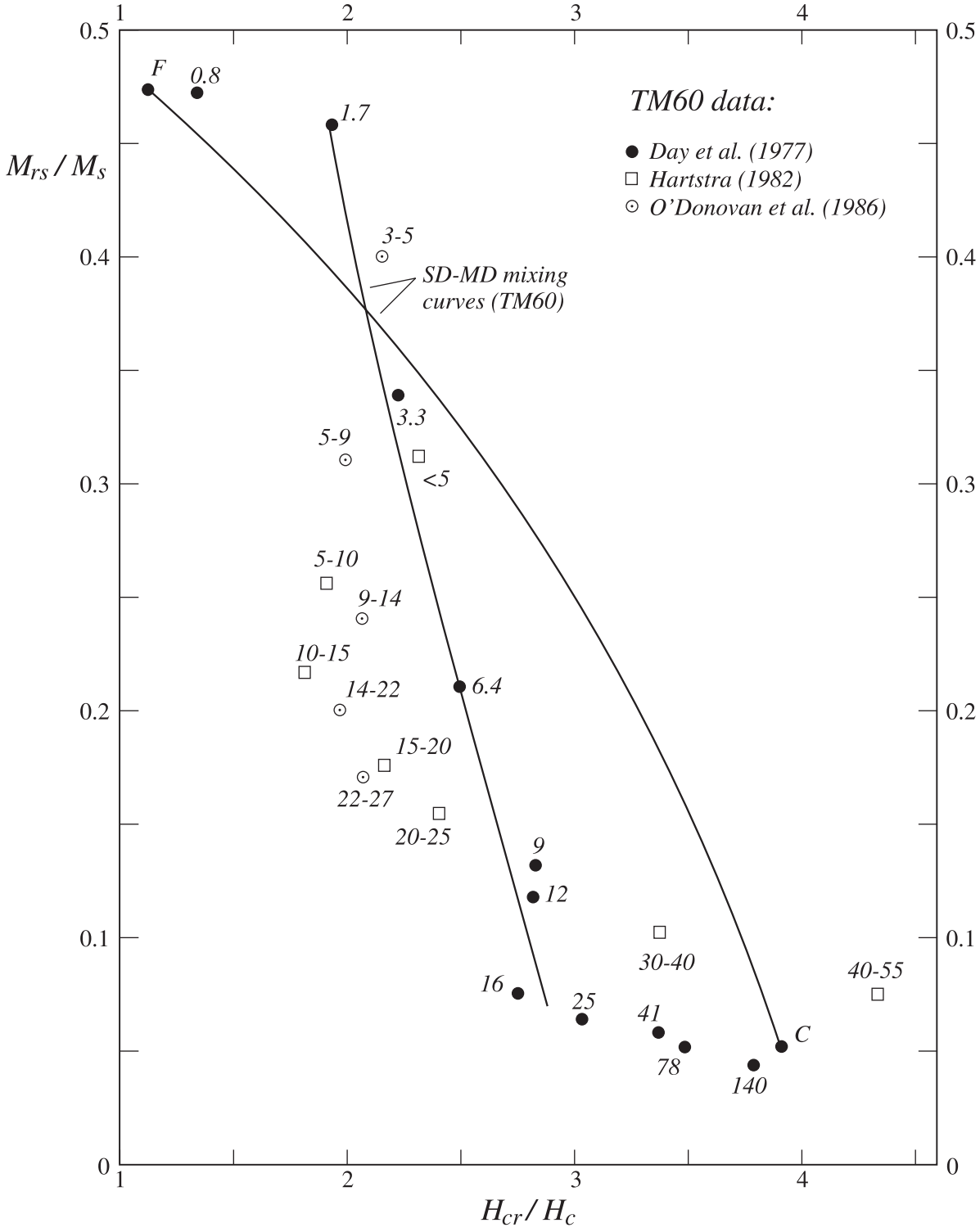

Figure 10. Data for sized TM60 grains from three different studies. Mixing coarse- and fine-grained end-member data (C, F) fails to explain the data. Numbers on data points are size spreads or mean grain sizes (in μm). Mixing data for 1.7-μm and 16- to 25-μm grains accounts for *Day et al.*'s [1977] data and in a more general way for the other data. The sharp descent in M_{rs}/M_s indicates a narrower transitional PSD range between SD and MD behavior than in magnetite.

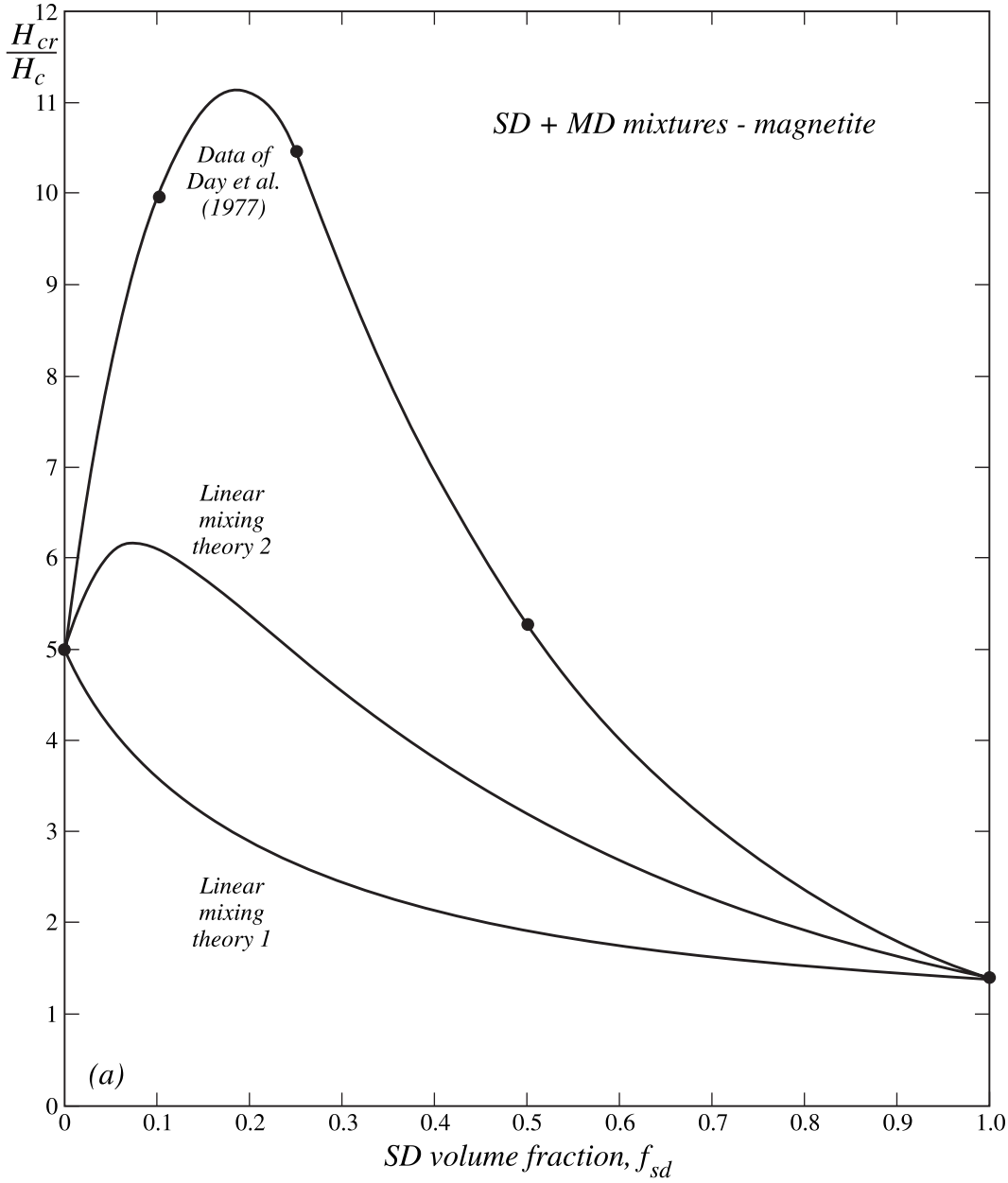

Figure 11. *Day et al.*'s [1977] H_{cr}/H_c data for bimodal mixtures of very coarse and very fine grains of (a) magnetite and (b) TM60. Nonlinear and modified linear mixing theories predict the observed peak in H_{cr}/H_c at intermediate f_{SD} values but underestimate its magnitude.

grains. Mixtures may require nonlinear calculations for H_{cr} and often for H_c as well. On the other hand, the PSD transition region is narrow for TM60 and the SD and MD end-members for mixing calculations are not greatly different in size or magnetic properties (Figure 10). A linear mixing model then works well for intermediate grain sizes (between 1.7 and 16 μm for Day et al.'s data). Once again, deviations into the bimodal region of the Day plot (Figure 12b) are unlikely in nature unless there are sources producing TM60 grains of greatly contrasting grain sizes, e.g., in chilled margins and adjacent coarser-grained interiors of pillow basalts.

4.5. Competing Roles of Grain Size and Stress

[50] In the PSD trend for magnetite, fine-grained samples tend to fall toward the SD end of the SD + MD mixing curves and coarser-grained samples toward the MD end (Figure 8a). Within any individual data set the progression of points along the curves is monotonic with grain size, but samples of similar size from different sets often have widely differing positions. Residual stress and/or the degree of imperfection of grains seems to be the other major factor determining remanence and coercivity ratios and thus position on the Day plot. In Figure 8b, hydrothermal magnetites with low internal stress and a high degree of crystallinity have low values of M_{rs}/M_s and high values of H_{cr}/H_c compared to chemically produced magnetites of similar size. In Figure 8d, points for annealed samples with reduced internal stress are displaced systematically toward lower M_{rs}/M_s and higher H_{cr}/H_c relative to points for their unannealed counterparts of the same size. Exactly the same trend is seen for hydrothermal magnetites and perfect single crystals in the MD data of Figure 3.

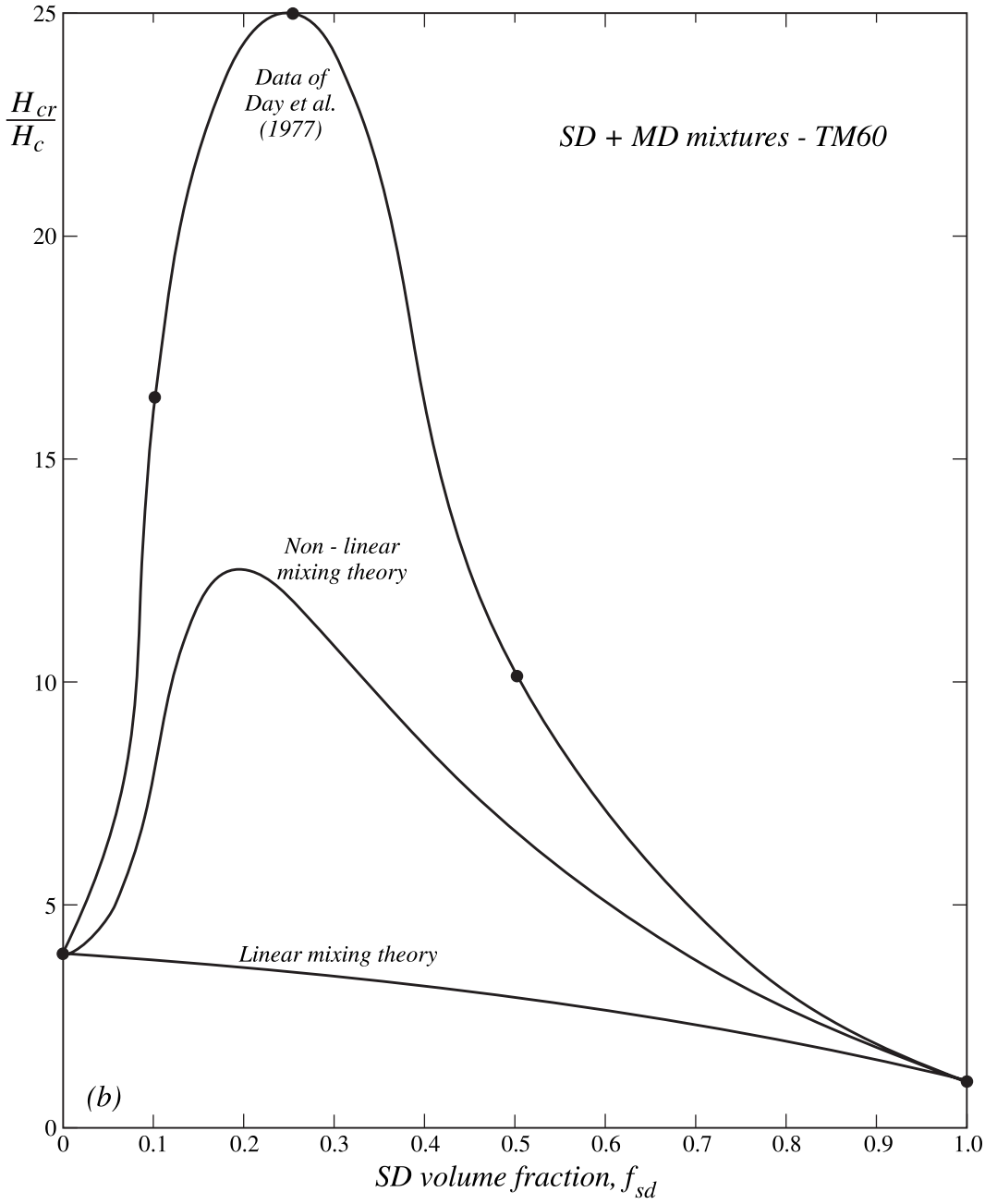

Figure 11. (continued)

4.6. PSD Data Trend for TM60

[51] The PSD data trend for TM60 is characterized by a fairly abrupt transition from SD to MD values of M_{rs}/M_s with only a small variation in H_{cr}/H_c, from 2 to 3 (Figure 10). Three data sets [*Day et al.*, 1977; *Hartstra*, 1982; *O'Donovan et al.*, 1986] agree that the PSD grain size range is narrower than in magnetite, extending from ≈2 to ≈25 μm.

[52] A narrower PSD size range for TM60 is not unexpected. The critical SD size for TM60 is predicted to be around 1–2 μm, compared to ≈0.1μm for magnetite. What is surprising is that H_{cr}/H_c varies so little while M_{rs}/M_s is changing by an order of magnitude. The roughly inverse relationship between M_{rs}/M_s and H_{cr}/H_c familiar from magnetite is absent in the PSD range of TM60. This contrast suggests a fundamental difference between the mechanism of PSD or transitional behavior in the two minerals. Although noisy, Day et al.'s data for other compositions of titanomagnetite suggest that $Fe_{2.8}Ti_{0.2}O_4$ (i.e., $x = 0.2$) behaves more or less like Fe_3O_4 ($x = 0$). The data for $Fe_{2.6}Ti_{0.4}$ ($x = 0.4$) are transitional between the magnetite and TM60 trends.

5. Conclusions

[53] The theory of M_{rs}/M_s and H_{cr}/H_c presented here, based mainly on linear approximations to magnetization and remanence curves, provides a first-order explanation of data trends on the *Day et al.* [1977] plot. A new region, for mixtures of superparamagnetic and stable SD grains, has been determined, with approximate limits $0.1 \leq M_{rs}/M_s \leq 0.5$ and $H_{cr}/H_c \leq 100$ (Figure 2). To use the linear or nonlinear theories for mixtures, a knowledge of M_s, M_{rs}, H_c, and

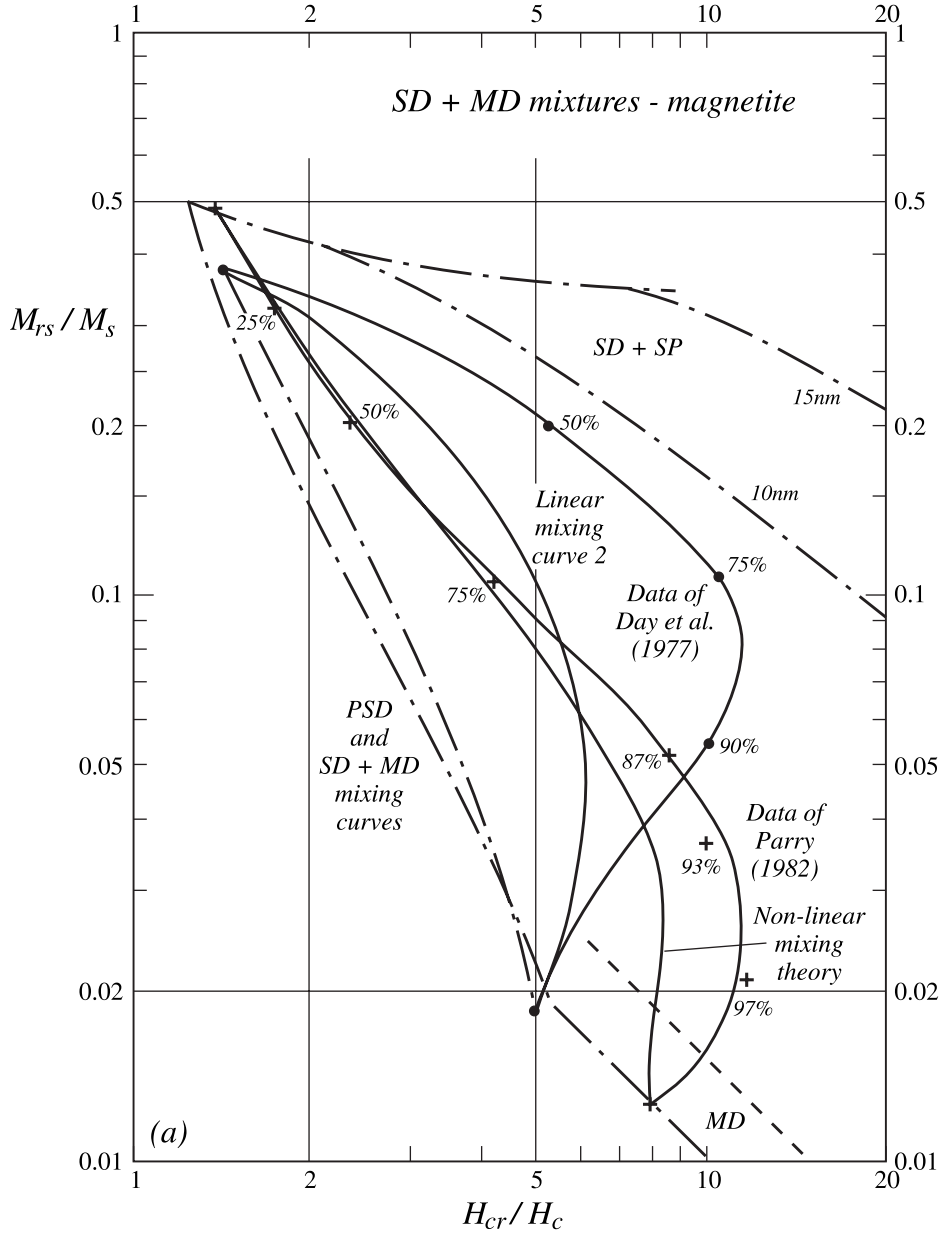

Figure 12. Experimental data for bimodal mixtures of (a) magnetite and (b) titanomagnetite grains from *Day et al.* [1977] and *Parry* [1982] compared with data for sized grains and with theoretical linear and nonlinear mixing curves. The bimodal data fall in a region of the Day plot between the linear SD + MD and SD + SP mixing curves, compromising the use of the Day plot for granulometry and domain state classification. The theoretical bimodal mixing curves fall in the same region as the data but underestimate the deviations of the data for both minerals from linear mixing curves and PSD data trends. Percentages are volume fractions of coarse MD material in each mixture.

H_{cr} for SD and MD end-members and χ_{SP} for SP grains is sufficient.

[54] MD grains of magnetite have a broad linear distribution of values on a log-log Day plot, from $M_{rs}/M_s \approx 0.02$ and $H_{cr}/H_c \approx 5$ to $M_{rs}/M_s \approx 0.001$ and $H_{cr}/H_c \approx 100$ (Figure 3). Larger grain size and/or weaker domain-wall pinning promotes low values of M_{rs}/M_s and high values of H_{cr}/H_c.

[55] Data for narrowly sized magnetites of PSD size are well described by curves for binary mixtures of SD and MD end-members (Figure 8). These curves are nonlinear on a log-log Day plot and intersect the MD trend.

[56] Although the SP + SD region of the Day plot remains to be tested with data for mixtures of controlled sizes, the predicted curves are very nonlinear. Linear regression fits to data for SP mixtures are not realistic. The only available data set, for mixtures of SP and PSD magnetites, agrees fairly well with theory if the average SP particle size is taken to be 9.3 nm (Figure 4). The actual particle size for the ferrofluid used in the mixtures is ≈10 nm.

[57] Bimodal mechanical mixtures of populations of grains with very different sizes and hysteresis parameters lead to unusual behavior. H_{cr}/H_c of the mixture is sometimes larger than H_{cr}/H_c of either separate population, and M_{rs}/M_s and H_{cr}/H_c data fall above PSD curves in a novel region of the Day plot (Figures 6, 11, and 12). In nature, only bimodal rocks with two very contrasting populations of magnetite or titanomagnetite grains (generally of different sources) will have these properties.

[58] The fact that a simple SD + MD mixture fits most data for well-sized PSD grains has fundamental implications. PSD

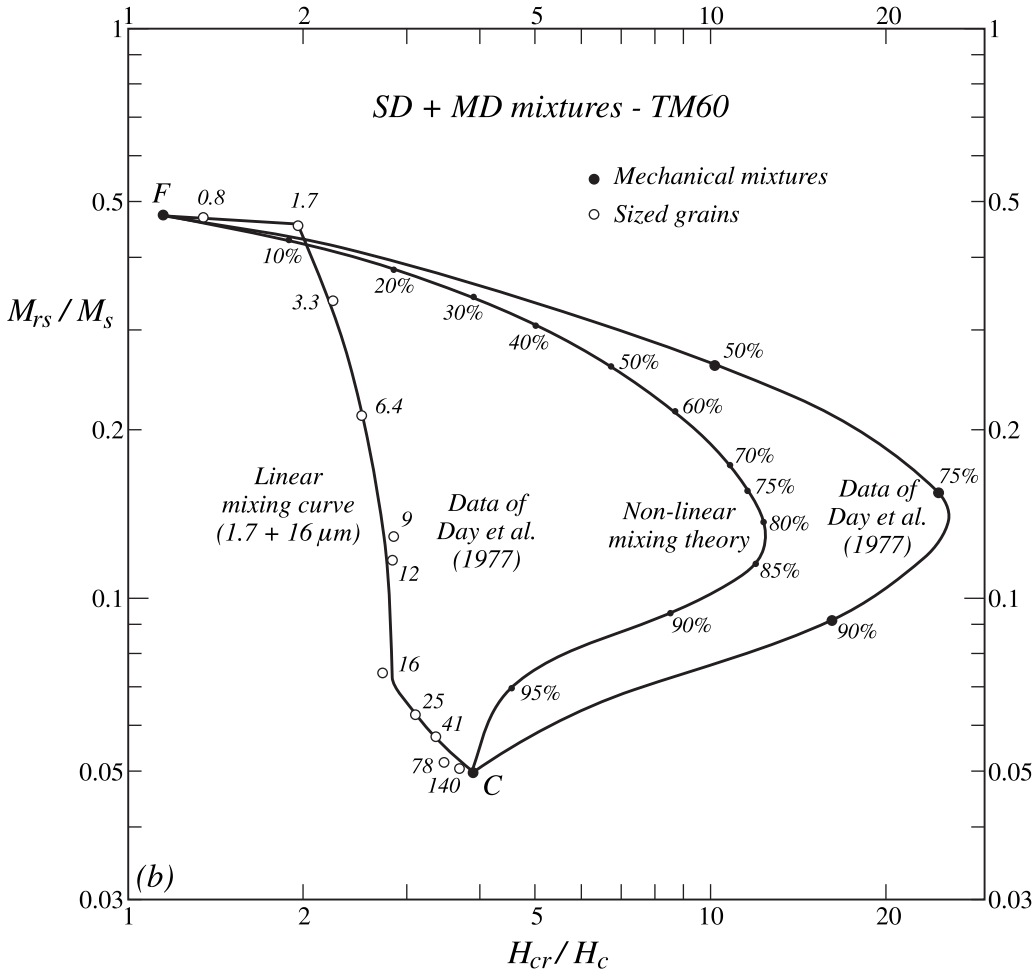

Figure 12. (continued)

behavior, in magnetite anyway, seems to be due to superposition of independent SD and MD moments whose properties do not vary greatly over a broad range of PSD grain sizes (see, however, *Roberts et al.* [2000] and Figure 10). Exotic structures like spin vortices are an unlikely explanation. Metastable SD grains [*Halgedahl and Fuller*, 1983] or domain imbalance moments [*Fabian and Hubert*, 1999] are a more probable source.

[59] Grain size and internal stress are competing factors in determining the position of points along the magnetite PSD and MD trends (Figures 8a, 8b, 8c, 8d, and 8e). Hydrothermally and chemically produced magnetites, with high and low degrees of crystal perfection, respectively, occupy contrasting positions even though their grain sizes match (Figure 8b). The same is true of annealed and unannealed magnetites (Figure 8d). In order to use the Day plot for granulometry, one must have independent information about levels of internal stress.

[60] Composition is also a factor. TM60 has a different distribution of points from magnetite. The PSD trend is narrower, more sharply delineated at the SD and MD ends, and occupies a different region in the Day plot (Figures 9 and 10). The PSD mechanism may be different than that of magnetite.

[61] **Acknowledgments.** I am grateful to Song Xu and Bruce Moskowitz for allowing me to use their data before publication and to Tilo von Dobeneck, Andrew Roberts, and Tim Rolph for helpful reviews. Work by Jeff Gee inspired me to construct a simple theory for the Day plot. This research was supported by the Natural Sciences and Engineering Research Council of Canada through grant A7709.

References

Argyle, K. S., and D. J. Dunlop, Low-temperature and high-temperature hysteresis of small multidomain magnetites (215-540 nm), *J. Geophys. Res.*, *95*, 7069–7083, 1990.

Carter, B. S., and B. M. Moskowitz, Magnetic parameters as a function of domain state and mixing ratio (abstract), *Eos Trans. AGU*, *80*(46), Fall Meet. Suppl., F300, 1999.

Channell, J. E. T., and C. McCabe, Comparison of magnetic hysteresis parameters of remagnetized and unremagnetized limestones, *J. Geophys. Res.*, *99*, 4613–4623, 1994.

Dankers, P., and N. Sugiura, The effects of annealing and concentration on the hysteresis properties of magnetite around the PSD-MD transition, *Earth Planet. Sci. Lett.*, *56*, 422–428, 1981.

Day, R., M. Fuller, and V. A. Schmidt, Hysteresis properties of titanomagnetites: Grain size and composition dependence, *Phys. Earth Planet. Inter.*, *13*, 260–267, 1977.

Dunlop, D. J., The hunting of the "psark", *J. Geomagn. Geoelectr.*, *29*, 293–318, 1977.

Dunlop, D. J., The rock magnetism of fine particles, *Phys. Earth Planet. Inter.*, *26*, 1–26, 1981.

Dunlop, D. J., Hysteresis properties of magnetite and their dependence on particle size: A test of pseudo-single-domain remanence models, *J. Geophys. Res.*, *91*, 9569–9584, 1986.

Dunlop, D. J., Thermoremanent magnetization of nonuniformly magnetized grains, *J. Geophys. Res.*, *103*, 30,561–30,574, 1998.

Dunlop, D. J., Theory and application of the Day plot (M_{rs}/M_s vs. H_{cr}/H_c), 2, Application to data for rocks, sediments and soils, *J. Geophys. Res.*, *107*, 10.1029/2001JB000487, 2002.

Dunlop, D. J., and Ö. Özdemir, *Rock Magnetism: Fundamentals and Frontiers*, 573 pp., Cambridge Univ. Press, New York, 1997.

Dunlop, D. J., M. F. Westcott-Lewis, and M. E. Bailey, Preisach diagrams and anhysteresis: Do they measure interactions?, *Phys. Earth Planet. Inter.*, *65*, 62–77, 1990.

Fabian, K., and A. Hubert, Shape-induced pseudo-single-domain remanence, *Geophys. J. Int.*, *138*, 717–726, 1999.

Fabian, K., A. Kirchner, W. Williams, F. Heider, T. Leibl, and A. Hubert, Three-dimensional micromagnetic calculations for magnetite using FFT, *Geophys. J. Int.*, *124*, 89–104, 1996.

Gee, J., and D. V. Kent, Calibration of magnetic granulometric trends in oceanic basalts, *Earth Planet. Sci. Lett.*, *170*, 377–390, 1999.

Halgedahl, S. L., and M. Fuller, The dependence of magnetic domain structure upon magnetization state with emphasis on nucleation as a mechanism for pseudo-single-domain behavior, *J. Geophys. Res.*, *88*, 6505–6522, 1983.

Hartstra, R. L., Grain-size dependence of initial susceptibility and saturation magnetization-related parameters of four natural magnetites in the PSD-MD range, *Geophys. J. R. Astron. Soc.*, *71*, 477–495, 1982.

Heider, F., D. J. Dunlop, and N. Sugiura, Magnetic properties of hydrothermally recrystalized magnetite crystals, *Science*, *236*, 1287–1290, 1987.

Heider, F., A. Zitzelsberger, and K. Fabian, Magnetic susceptibility and remanent coercive force in grown magnetite crystals from 0.1 μm to 6 mm, *Phys. Earth Planet. Inter.*, *93*, 239–256, 1996.

Hodych, J. P., Magnetic hysteresis as a function of low temperature in rocks: Evidence for internal stress control of remanence in multidomain and pseudo-single-domain magnetite, *Phys. Earth Planet. Inter.*, *64*, 21–36, 1990.

Jackson, M., Diagenetic source of stable remanence in remagnetized Paleozoic cratonic carbonates: A rock magnetic study, *J. Geophys. Res.*, *95*, 2753–2762, 1990.

King, J., S. K. Banerjee, J. Marvin, and Ö. Özdemir, A comparison of different magnetic methods for determining the relative grain size of magnetite in natural materials, *Earth Planet. Sci. Lett.*, *59*, 404–419, 1982.

Nagata, T., and B. J. Carleton, Magnetic remanence coercivity of rocks, *J. Geomagn. Geoelectr.*, *39*, 447–461, 1987.

Newell, A. J., and R. T. Merrill, Size dependence of hysteresis properties of small pseudo-single-domain grains, *J. Geophys. Res.*, *105*, 19,393–19,403, 2000.

O'Donovan, J. B., D. Facey, and W. O'Reilly, The magnetization process in titanomagnetite ($Fe_{2.4}Ti_{0.6}O_4$) in the 1–30 μm particle size range, *Geophys. J. R. Astron. Soc.*, *87*, 897–916, 1986.

Özdemir, Ö., and S. K. Banerjee, A preliminary magnetic study of soil samples from west-central Minnesota, *Earth Planet. Sci. Lett.*, *59*, 393–403, 1982.

Özdemir, Ö., and D. J. Dunlop, Effect of crystal defects and internal stress on the domain structure and magnetic properties of magnetite, *J. Geophys. Res.*, *102*, 20,211–20,224, 1997.

Özdemir, Ö., and D. J. Dunlop, Single-domain-like behavior in a 3-mm crystal of magnetite, *J. Geophys. Res.*, *103*, 2549–2562, 1998.

Özdemir, Ö., S. Xu, and D. J. Dunlop, Closure domains in magnetite, *J. Geophys. Res.*, *100*, 2193–2209, 1995.

Parry, L. G., Magnetic properties of dispersed magnetite powders, *Philos. Mag.*, *11*, 303–312, 1965.

Parry, L. G., Shape-related factors in the magnetization of immobilized magnetite particles, *Phys. Earth Planet. Inter.*, *22*, 144–154, 1980.

Parry, L. G., Magnetization of immobilized particle dispersions with two distinct particle sizes, *Phys. Earth Planet. Inter.*, *28*, 230–241, 1982.

Pike, C. R., A. P. Roberts, and K. L. Verosub, Characterizing interactions in fine magnetic particle systems using first order reversal curves, *J. Appl. Phys.*, *85*, 6660–6667, 1999.

Rahman, A. A., A. D. Duncan, and L. G. Parry, Magnetization of multi-domain magnetite particles, *Riv. Ital. Geofis.*, *22*, 259–266, 1973.

Roberts, A. P., Y. Cui, and K. L. Verosub, Wasp-waisted hysteresis loops: Mineral magnetic characteristics and discrimination of components in mixed magnetic systems, *J. Geophys. Res.*, *100*, 17,909–17,924, 1995.

Roberts, A. P., C. R. Pike, and K. L. Verosub, First-order reversal curve diagrams: A new tool for characterizing the magnetic properties of natural samples, *J. Geophys. Res.*, *105*, 28,461–28,475, 2000.

Schmidbauer, E., and R. Keller, Magnetic properties and rotational hysteresis of Fe_3O_4 and γ-Fe_2O_3 particles 250 nm in diameter, *J. Magn. Magn. Mater.*, *152*, 99–108, 1996.

Schmidbauer, E., and N. Schembera, Magnetic hysteresis properties and anhysteretic remanent magnetization of spherical Fe_3O_4 particles in the grain size range 60-160 nm, *Phys. Earth Planet. Inter.*, *46*, 77–83, 1987.

Smirnov, A. V., and J. A. Tarduno, Low-temperature magnetic properties of pelagic sediments (Ocean Drilling Program Site 805C): Tracers of maghemitization and magnetic mineral reduction, *J. Geophys. Res.*, *105*, 16,457–16,471, 2000.

Stacey, F. D., A generalized theory of thermoremanence, covering the transition from single domain to multi-domain magnetic grains, *Philos. Mag.*, *7*, 1887–1900, 1962.

Stacey, F. D., and S. K. Banerjee,, *The Physical Principles of Rock Magnetism*, 195 pp., Elsevier Sci., New York, 1974.

Suk, D., and S. L. Halgedahl, Hysteresis properties of magnetic spherules versus whole-rock specimens from some Paleozoic platform carbonates, *J. Geophys. Res.*, *101*, 25,053–25,075, 1996.

Tauxe, L., T. A. T. Mullender, and T. Pick, Pot-bellies, wasp-waists and superparamagnetism in magnetic hysteresis, *J. Geophys. Res.*, *101*, 571–583, 1996.

Thompson, R., Can we mathematically unmix natural magnetic mixtures? (abstract), *Int. Union Geod. Geophys. Gen. Assembly Abstr.*, *XXII*, A318, 1999.

Williams, W., and D. J. Dunlop, Simulation of magnetic hysteresis in pseudo-single-domain grains of magnetite, *J. Geophys. Res.*, *100*, 3859–3871, 1995.

D. J. Dunlop, Geophysics, Physics Department, University of Toronto, Toronto, Ontario, Canada M5S 1A7. (dunlop@physics.utoronto.ca)